Chalmers University of Technology

# On finding optimal machines and comparison of axial and radial flux propulsion machines

**MIKAEL ALATALO**

**DEPARTMENT OF Electrical Engineering**

CHALMERS UNIVERSITY OF TECHNOLOGY
Gothenburg, Sweden 2021
www.chalmers.se

**On finding optimal machines and comparison of axial and radial flux propulsion machines**

© M. Alatalo 2021

Technical report 2021:2
Department of Electrical Engineering
Division of Electric Power Engineering
CHALMERS UNIVERSITY OF TECHNOLOGY
SE-412 96 Gothenburg
Sweden, 2021

## Abstract

Permanent magnet synchronous motors are often used in drive trains for electric and hybrid vehicles. At the Division of Electrical Engineering at Chalmers University of Technology, several works on different machine types as traction motor have been done. Radial flux machines of different sizes, axial and transversal machines have been investigated. Together with the department of Environmental Systems Analysis, the different motors have also been objects for LCA calculations.

A method for calculating the axial flux machine is investigated. The 3D-analysis is replaced by five 2D-calculations for different radii. The resulting torque is estimated correctly with the 2D approximation but there are bigger differences to the eddy current losses. The method is used for analysis of an axial flux machine with central stator and two rotor discs. A method for finding a useful machine for propulsion is tested where maximum torque, field weakening, and high efficiency are key parameters. A radial flux machine with 8-poles is compared to the best axial flux machines.

To find a good size, pole number etc., a method with randomised parameters and a multitude of calculations are done. The selection of machine constructions is done based on data from a few operational points. Afterwards, some selected machines, that in steps are changed towards better performance, are evaluated both in terms of mapped efficiency and calculated performance during WLTP, US06 and other drive cycles.

The best investigated axial flux machine can produce 20 % lower losses than the reference machine, in the low-speed drive cycles, if grain-oriented laminations are used in the stator teeth. At higher speed drive cycles, the losses are 20 % higher than from the radial flux machine. If a thinner lamination will be used, the losses could be lowered in the high-speed region.

The weight of the axial flux machine can be lower than of the radial flux machine, but if the efficiency shall be better or equal, the weight of the axial flux machine will be higher.



## Acknowledgements

This work has been financed by Swedish Electromobility Centre, which is gratefully acknowledged. Sonja Lundmark has patiently helped me with the report, thanks Sonja.

# Contents

Abstract ..... 3
1. Introduction ..... 7
2. 2D versus 3D ..... 9
    2.1 Distributed winding ..... 9
    2.2 Concentrated winding ..... 12
3. Reference motor for comparison to the axial flux machine ..... 15
4. Drive cycles and car model ..... 17
    4.1 WLTP ..... 17
    4.2 US06 ..... 18
    4.3 'Kassel' hills ..... 18
    4.4 Highway speed ..... 19
5. Results in terms of efficiency ..... 21
    5.1 Permanent magnet radial flux machine ..... 21
    5.3 Axial flux machine design approach ..... 22
    5.4 Axial flux machine with alternative rotor ..... 29
    5.5 Axial flux machine with grain-oriented material ..... 35
    5.6 Axial flux machine with toroidal winding ..... 41
6. Results from drive cycle evaluations and comparison to 3D ..... 45
    6.1 Drive Cycles ..... 45
    6.2 Comparison to 3D ..... 46
7. Rotor core ..... 49
8. Conclusion ..... 51
9. Future work ..... 53
References ..... 55
Appendix A. Slot and rotor pole ..... 57
    Appendix A.1 Rotor of concentrated winding ..... 57
Appendix B. Programs that are used. ..... 59
Appendix C Material data ..... 61
Appendix D Summary of machine data ..... 63

# 1. Introduction

Axial flux machines are investigated as traction motor for electric vehicles. The axial flux machine can be built in several ways, see [4], but this report focuses on the variant with a central stator and two rotor discs. The central stator doesn't need any return path for the flux and the weight and losses are minimised. As the magnetic flux pass the stator in the axial direction, grain-oriented steel may be used. There are several benefits with the axial flux machine, but one drawback is the overall winding length. There are also challenges when mounting and cooling the stator.

To analyse the motor, 3D-FEM has to be used in order to get a good understanding of the construction. As an alternative, 2D-FEM is used for several radii. This has earlier been investigated by [1-3] and a good approximation of the 3D solution can be found both with analytical and 2D-methods. Parviainen et.al. found that the analytical model resulted in too high flux density, and this was probably due to an assumed linear iron core material. This work focuses on machines for electric vehicles, and it is assumed that they are heavily loaded with high current density as well as high flux density. The core material will saturate and of that reason, the analytical method is assumed to have too large errors and the focus is on the 2D-FEM method. In [3], they also found that evaluation at 5 different radii gave a good result, except for the cogging torque.

Gair et.al. [1] Found that a 2D-analysis for four radii gave a good result, especially if the end effects of the windings are added.

Earlier work at the Department of Electrical Engineering have focused on the central stator construction which are used by Yasa and Magnax, [4-5]. LCA-calculations have been done and compared to other machine types. The central stator has no back iron which results in low weight and low core losses. The efficiency hasn’t been good enough when the radius is limited. It has been evaluated on the basis with the same outer radius as other machines but in this work the radius can be freely chosen. The loss in the rotor is a problem at high current loading, concentrated windings and high speed. The combination of concentrated windings and surface mounted magnets are common in the axial flux machines (AFM) and the magnets are sensitive to the applied flux density from the stator side.

The efficiency of the propulsion system is important of several reasons. The energy loss during driving is perhaps not the biggest issue, renewable energy is fairly cheap today, and a high consumption doesn't show in the money spent. However low efficiency put high demand on battery size and charging infrastructure. An efficient use of produced batteries and infrastructure makes it easier the coming decades when the transportation sector must transform to zero carbon dioxide.

Axial flux machines using grain-oriented iron core is investigated. The flux density through a centre stator is mainly directed in the axial direction so there is an opportunity to reduce the iron core losses of the stator. Grain oriented laminations are used in 50/60 Hz transformers where a lot of efforts are made to lower the losses in this material, [8-10]. As the frequency is quite low in the transformers, the focus is on the hysteresis losses of the material. When used in traction motors with a fundamental frequency close to 1 kHz the eddy current losses will be a problem due to thicker laminations (compared no non-oriented iron).

# 2. 2D versus 3D

## *2.1 Distributed winding*

A method where the 3D-calculation is replaced by 2D along the circumferential length of five different radii is investigated. The 3D calculation is done with Ansys Maxwell and the one-sided machine can be seen in Figure 1.

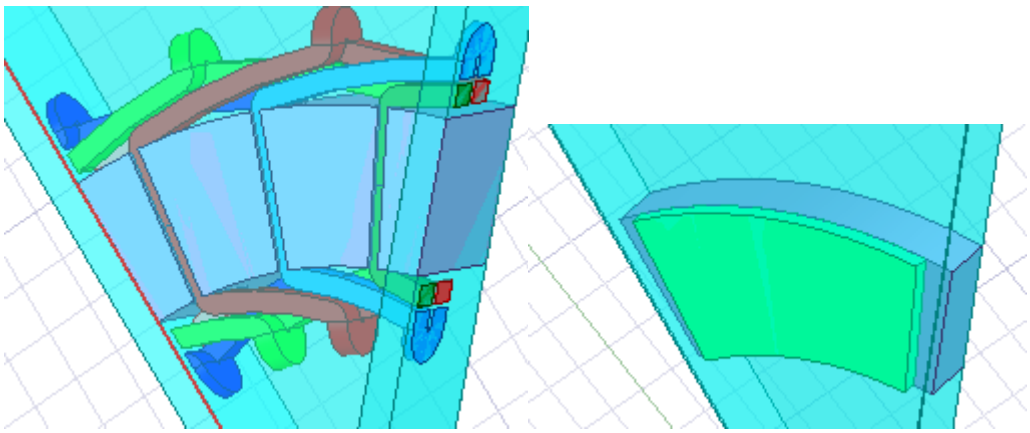

Figure 1.a. Stator of distributed winding. b. Rotor

The slot can be seen in Figure 2.a and the pole in Figure 2.b. The lossless material is only for calculations. One part of the stator and one rotor is shown, and the machine should repeat itself instead of the lossless material. More machine data, and results, are seen in Tables 1 to 5.

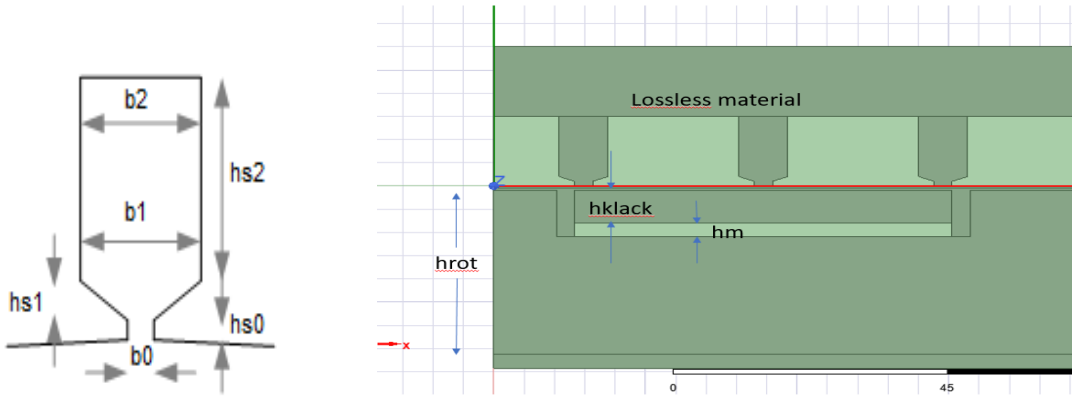


Figure 2. a) Investigated slot and b) pole

Table 1. Main data of machine

| | |
|---|---|
| Outer diameter | 200 mm |
| Inner diameter | 140 mm |
| Air gap | 1 mm (per side) |
| Number of poles | 8 |
| Number of slots | 24 |
| Stator length | 30 mm |
| Rotor length | 10 mm |
| Core material | NO30 |

Table 2. Slot data

| | |
|---|---|
| b0 | 2 mm |
| b1 | 5 mm |
| b2 | 5 mm |
| hs0 | 1 mm |
| hs1 | 1 mm |
| hs2 | 15 mm |

Table 3. Winding and magnet data

| | |
|---|---|
| Magnet thickness | 3 mm |
| Magnet width | 85 % of pole |
| Magnet material | NMX-37 100 degC |
| Number of turns | 10 per slot |
| Fill factor | 51 % |
| Cu weight | 0.96 kg |
| Turn length | 216 mm |
| Copper diameter | 1.63 mm |

Table 4. Results from 3D and 3600 rpm

| | $i_d=0$, $i_q=0$ | $i_d=0$, $i_q=241$ Arms | $i_d=-241$, $i_q=0$ Arms | $i_d=0$, $i_q=241$ Arms finer mesh |
|---|---|---|---|---|
| Torque ( Nm ) | 0 | 75 | 0 | 75 |
| Psid ( Wb) | 0.0457 | 0.0362 | -0.0475 | 0.0362 |
| Psiq ( Wb) | 0 | 0.0738 | 0 | 0.0734 |
| Peddy | 22 W | 85 W | 32 W | 83 W |
| Physt | 27 W | 99 W | 42 W | 100 W |
| Pcu | 0 | 6.76 kW | 6.76 kW | 6.76 kW |

In the last column in Table 4, a reference result is calculated with finer mesh, but the result doesn't diverge compared with the first calculations. The first calculations are done with standard mesh values which is used further on in the report.

As a comparison, the data from 2D analysis at radii = 73, 79, 85, 91 and 97 mm is used for approximation of the 3D-pole.

Table 5. Results from 2D.

| | $i_d=0$, $i_q=0$ | | | $i_d=0$, $i_q=241$ Arms | | | $i_d=-241$, $i_q=0$ Arms | | |
|---|---|---|---|---|---|---|---|---|---|
| | *2D* | *3D* | *difference* | *2D* | *3D* | *difference* | *2D* | *3D* | *difference* |
| Torque ( Nm ) | 0 | 0 | 0% | 80,8 | 75 | 8% | 0 | 0 | 0% |
| Psid ( Wb) | 0,0457 | 0,0457 | 0% | 0,0404 | 0,0362 | 12% | -0,0244 | -0,0475 | -49% |
| Psiq ( Wb) | 0 | 0 | 0% | 0,0612 | 0,0738 | -17% | 0 | 0 | 0% |
| Peddy (W) | 19 | 22 | -14% | 50 | 85 | -41% | 15 | 32 | -53% |
| Physt (W) | 32 | 27 | 19% | 87 | 99 | -12% | 23 | 42 | -45% |
| Pcu (kW) | | 0 | | | 6,76 | | | 6,76 | |

The torque calculation differs 7.7 percent and the 2D eddy current losses are underestimated compared to the 3D calculation, see Table 5. The difference is particularly high for the field weakening point ($i_d$=-241, $i_q$=0 Arms). The copper loss is only calculated for the active machine and the end windings are dominating the overall length. When calculating the copper loss, the end windings must be added to the 2D-calculation. The leakage flux from the winding has to be added and as the machine have long end windings, the leakage should be added. In this study it is however neglected.

## *2.2 Concentrated winding*

A concentrated winding is also considered. In this case the winding is closer to the core, see Figure 3.

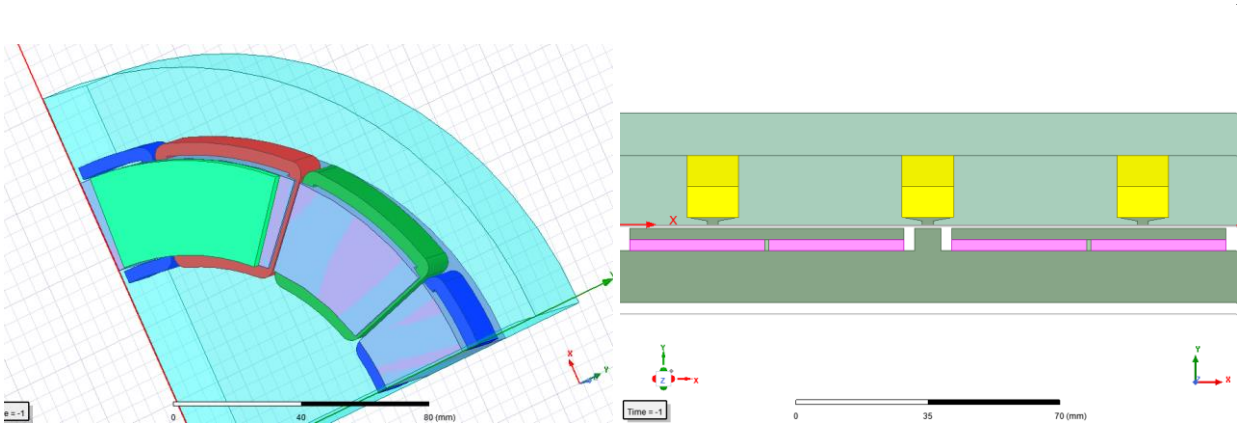

a) b)

Figure 3. Concentrated winding. a) 3D, rotor core and one magnet are hidden. b) 2D

Table 6. Main data of machine

| | |
|---|---|
| Outer diameter | 200 mm |
| Inner diameter | 140 mm |
| Air gap | 1 mm (per side) |
| Number of poles | 8 |
| Number of slots | 12 |
| Stator length | 30 mm |
| Rotor length | 10 mm |
| Core material | NO30 |

Table 7. Slot data

| | |
|---|---|
| b0 | 2 mm |
| b1 | 10 mm |
| b2 | 10 mm |
| hs0 | 1 mm |
| hs1 | 1 mm |
| hs2 | 10 mm |

Table 8. Winding and magnet data

| | |
|---|---|
| Magnet thickness | 3 mm |
| Magnet width | 85 % of pole |
| Magnet material | NMX-37 |
| Number of turns | 20 per slot |
| Fill factor | 50,00% |
| Cu weight | 0.62 kg |
| Turn length | 140 mm |
| Copper diameter | 1.63 mm |
| No. parallel con | 2 |
| $R_s$ ( Maxwell) | 33 mΩ |

Table 9. Results from 3D

| | $i_d=0$, $i_q=0$ | $i_d=0$, $i_q=241$ Arms | $i_d=-241$, $i_q=0$ Arms |
|---|---|---|---|
| Torque ( Nm ) | 0 | 67 | 0 |
| Psid ( Wb) | 0.0415 | 0.0325 | -0.050 |
| Psiq ( Wb) | 0 | 0.0730 | 0 |
| Peddy | 18 W | 88 W | 57.5 W |
| Physt | 28 W | 100 W | 42 W |
| Pcu | 0 | 3.83 kW | 3.83 kW |

Table 10. Results from 2D

| | $i_d=0$, $i_q=0$ | | | $i_d=0$, $i_q=241$ Arms | | | $i_d=-241$, $i_q=0$ Arms | | |
|---|---|---|---|---|---|---|---|---|---|
| | *2D* | *3D* | *difference* | *2D* | *3D* | *difference* | *2D* | *3D* | *difference* |
| Torque ( Nm ) | 0 | 0 | 0% | 65 | 67 | -3% | 0 | 0 | 0% |
| Psid ( Wb) | 0,0409 | 0,0415 | 0% | 0,037 | 0,0325 | 14% | -0,032 | -0,05 | -36% |
| Psiq ( Wb) | 0 | 0 | 0% | 0,063 | 0,073 | -14% | 0 | 0 | 0% |
| Peddy (W) | 16 | 18 | -11% | 54 | 88 | -39% | 25 | 57,5 | -57% |
| Physt (W) | 30 | 28 | 7% | 86 | 100 | -14% | 38 | 42 | -10% |
| Pcu (kW) | | 0 | | | 3,83 | | | 3,83 | |

The result is quite good and believed to be useful as a first approximation of the actual machine. In 2D, the losses are underestimated which could be a result of the neglected end winding. This is

mentioned in [3] where compensation of the end winding is used in order to get good results. This could be something to consider even in radial flux machines that have short axial length and wide pole pitches.

The 2D-analysis with five different radii occupies 2 min and 25 seconds on my computer. The 3D-analysis must run for 62 minutes per operating point. The 2D-version can be used for a much quicker result when dimensioning axial flux machines.

# 3. Reference motor for comparison to the axial flux machine

The base for this work is a variant of the Toyota Prius machine from 2004. Smaller alterations to the Prius solution are made and it is called the reference machine. It is used as reference machine in many types of studies at the Division of Electric Power Engineering. An illustration of the machine is shown in Figure 4.

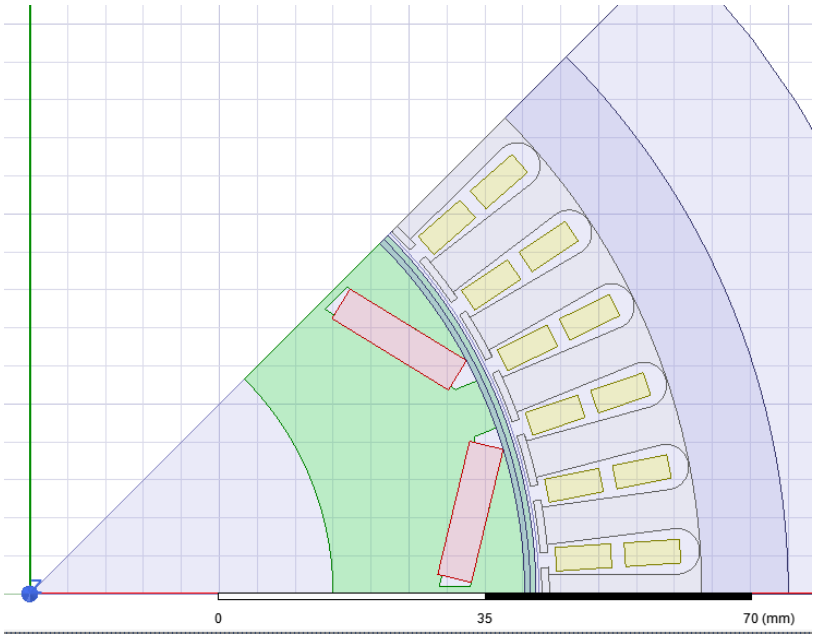


Figure 4. Reference motor. Outer diameter 200 mm.

Different approaches have earlier been used when doing comparison between different machine types. The latest done in [6] have fixed outer diameter, air gap and current density. In this work the parameters are free to choose as well as slot shape, magnet thickness and so on. Different rotor constructions are also investigated.

# 4. Drive cycles and car model

Several drive cycles are at hand for evaluation, see [1]. In this report I've limited the evaluation to two drive cycles and one invented. The loss during pure highway use is also evaluated.

The main car data are shown in Table 11. They are the same as in [14].

Table. 11 Car data

| | |
|---|---|
| Car mass ( kg) | 1700 |
| $C_d$ value | 0.29 |
| Front area ($m^2$) | 1,9 |
| Top speed ( km/h) | 140 |
| Gearing motor to speed | 12000 / 140 (rpm/km/h) |
| DC-link voltage ( V ) | 430 |

## *4.1 WLTP*

WLTP is the certifying drive cycle of European cars and an important measure for new vehicles. The acceleration is fairly low, and the torque demand implies a motor power of 60-75 kW for a normal car. The high-speed part of the drive cycle increases this figure, but overall, the power is fairly low and represents every day travelling with normal driving.

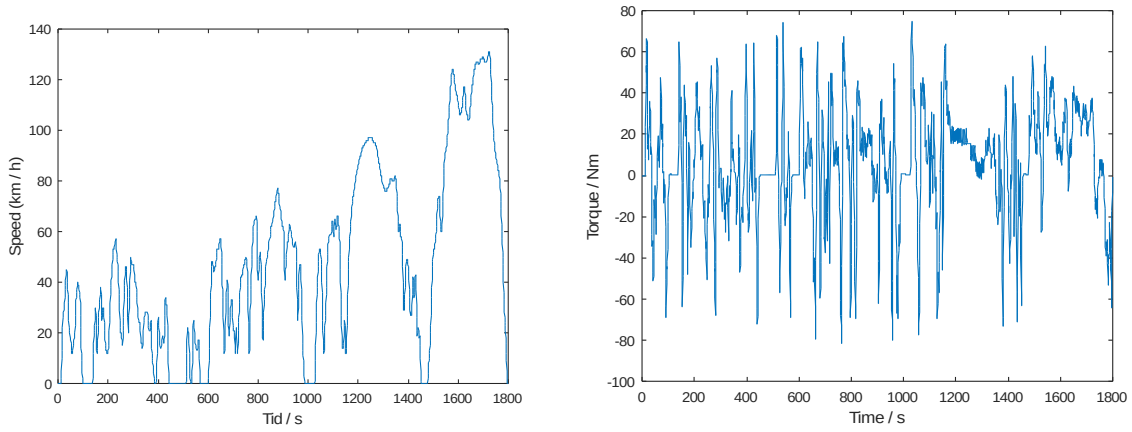


Figure 5.a. WLTP speed vs time. b. Torque vs time

The mean value of the speed is 45.5 km/h, which corresponds to 3500 rpm if the top speed of the motor is reached at 140 km/h.

Figure 5.b shows the resulting torque on the vehicle and median value of the torque is 16.3 Nm while the mean value is 20.7 Nm, i.e., quite low values.

The drive cycle covers 23.2 km, and the cycle is divided in four parts, LOW, MEDIUM, HIGH and EXTRA HIGH, [7].

The peak acceleration is approximately 1.5 $m/s^2$.

## *4.2 US06*

The drive cycle US06 is a highway cycle with rather high acceleration. Figure 6 shows the speed during the cycle.

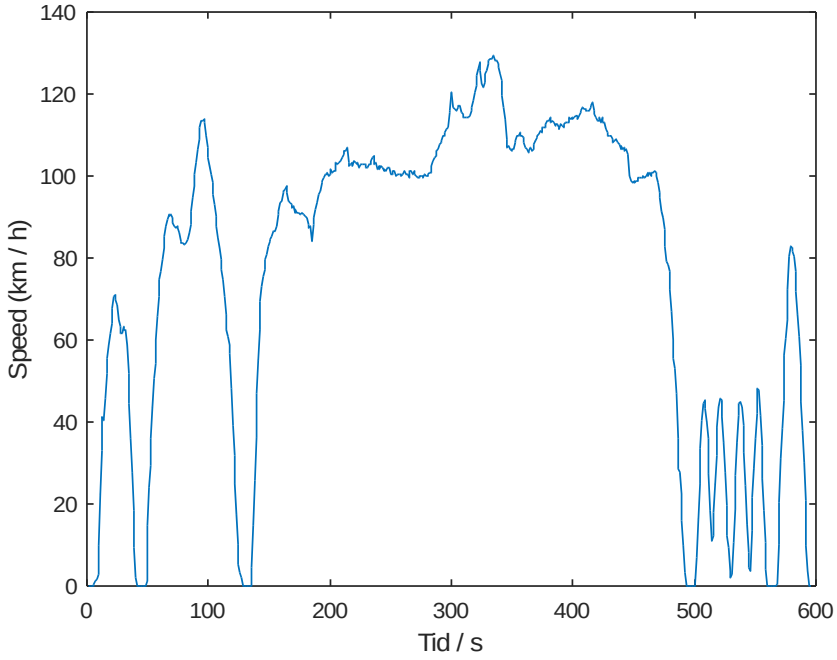


Figure 6. US06 speed in km/h.

The drive cycle covers 12.9 km, and the cycle ends with repeated accelerations.

## *4.3 'Kassel' hills*

This drive cycle is invented partly because of own experience when travelling with my -09 Prius in 140 km/h. I found that the battery was empty at the top of the hills. Colleagues at VCC told me that the part of highways is extra demanding. It consists of repeated up and downs, and when travelling at high speed, the power is high. I've assumed a slope of 8 % and an elevation of 300 m. It's worth noting that hardly any parts of Swedish interregional ways exceed 6 %.

I've assumed a constant speed of 120 km/h and then the slope changes resulting in a varying torque, see Figure 7. The drive cycle covers 49.9 km and starts with an acceleration up to 120 km/h.

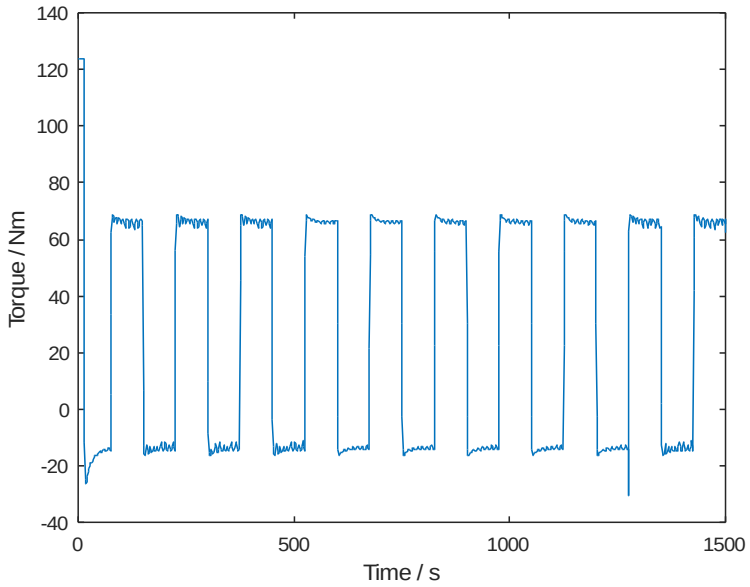


Figure 7. Torque when max speed is 120 km/h.

## *4.4 Highway speed*

My opinion is that the efficiency at highway speed is important. If you buy a modern electric vehicle and intend to use it for more than city-driving, the behaviour at highway speed is important. The major route in Sweden have the speed limit of 110 km/h and 120 km/h. Interregional ways have a lower tempo between 80-100 km/h so one could discuss which speed is the most relevant. I think 120 is a good point for investigation for two reasons.

1. If it's not clear for the costumer, an electric car behaves different to ICE cars. The latter increase efficiency when speed and torque increase, which disguise the vehicle consumption. The difference between 90 km/h and 120 km/h can be as high as 100 % in an electric vehicle. There is a clear risk for disappointed costumers that buy an expensive big car with big battery but the resulting range at highway speed is 250-300 km, when the WLTP range is over 450 km. If that is paired with low charge power the result is not good.
2. The second reason is of course energy use. Electric energy is not so costly but when the number of vehicles grow, the demand on electric grid and energy production will grow as well. So, an overall awareness of the consumption is nice especially the coming decades when the number of electric vehicles will grow and we have to increase the output from battery manufacturers, charging infrastructure and electric grid.

# 5. Results in terms of efficiency

## *5.1 Permanent magnet radial flux machine*

The efficiency mapping of the reference motor is shown in Figure 8. The machine has over 94 % efficiency from as low as 20 Nm and the efficiency is high at high rotational speed.

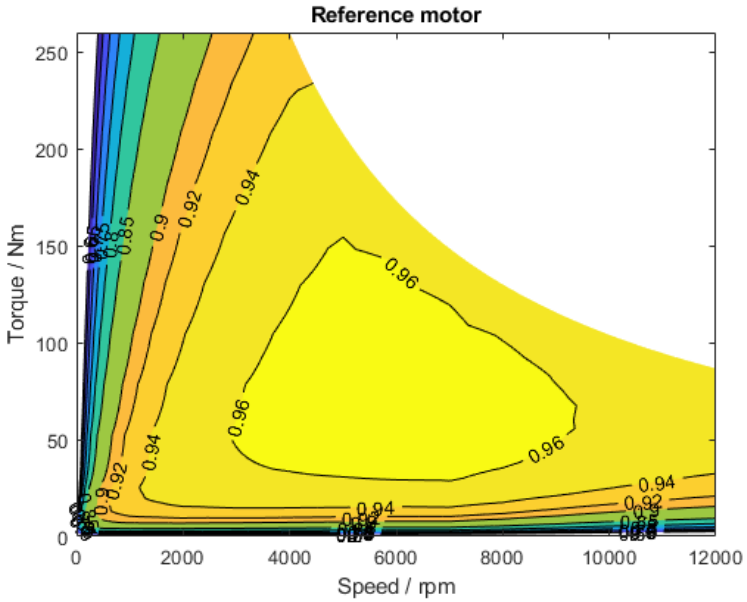


Figure 8. Efficiency at different speed and torque of a PM-machine. Reference motor.

The machine is the same as in [1] but, the so-called reference motor that is used frequently at the Electric Department on Chalmers University. In this work where a radial flux machine is compared to the axial flux machines, 100 °C is used for the winding temperature and the MTPA-method is used for finding an operational point. The maximum torque and current to this machine are little bit higher than the other machines but no evaluation point exceeds 240 Nm.

The resulting WLTP-losses of this machine is 1.191 kWh / 100 km.

Main data of this machine are shown in Table 12.

Table 12. Main data of reference machine

| | |
|---|---|
| Outer diameter | 200 mm |
| Inner diameter | 135 mm |
| Air gap | 0.75 mm |
| Number of poles | 8 |
| Number of slots | 48 |
| Stator length | 127 mm |
| Rotor length | 127 mm |

| | |
|---|---|
| Core material | NO30 |
| Voltage | 292 V |
| Phase Current | 286 A |

Table 13. Slot data

| | |
|---|---|
| Acu, slot | 101 mm2 |
| Tooth width | 5 mm |
| Slot opening | 2 mm |

Table 14. Winding and magnet data

| | |
|---|---|
| Magnet thickness | 4.6 mm |
| Magnet width | 18 mm |
| Magnet material | NMX-37 |
| Magnet temp | 70 °C |
| Number of turns | 8 per slot |
| Fill factor | 45,00% |
| No. parallell con | 4 |
| Mcu | 4.8 kg |
| Mstator | 11.8 kg |
| Mnd | 1.25 kg |
| Mrotor | 7.4 kg |
| Jcu @ 240 Nm | 20 A/mm2 |

## *5.3 Axial flux machine design approach*

The axial flux machine is analysed using the approximative 2D-method and the goal is to optimise the machine over the WLTP-drive cycle and other drive cycles. The goal is to find an optimal machine with the lowest losses during the drive cycle.

As a start, it is assumed that the optimal machine can be found between the outer radius100 mm to 200 mm. The slot depth for one part is assumed to be between 7 and 20 mm. The slot width is varied between 7 and 20 mm as well. The pole numbers are varied between 8, 10, 12 to 16 poles and the magnet thickness can be varied between 2-4.5 mm.

Using the function rand in Matlab, the outer radius, slot width, slot depth, pole number and magnet

thickness are varied in a randomised manner.

A selection of suitable machines is found in two steps. First, a selection of machines that can produce 240 Nm and are able to be used in field weakening. From a created design of one half of the magnet, the magnet flux is calculated and from that flux, the current for producing 120 Nm is calculated. Since some machines are heavily loaded, they are nonlinear and will not be able to produce 120 Nm with the calculated current. A limit is introduced and that is machines that produce lower than 100 Nm are scrapped. Machines that have too low or too high flux in q-direction are also scrapped. Machines having too high flux will need to have high d-direction current when field weakened, and machines having too low flux will need extra current for producing the max torque.

Using semi random values for radius, slot shape, magnet thickness and pole numbers result in solutions with different weight and losses. In Figure 11, the solutions are shown with mass and losses of each solution.

For each solution, the flux without current is calculated and from that the necessary iq can be calculated. This doesn't always work, so some of the solutions aren't valid.

As a start, machines that fulfil the first two requests are found.

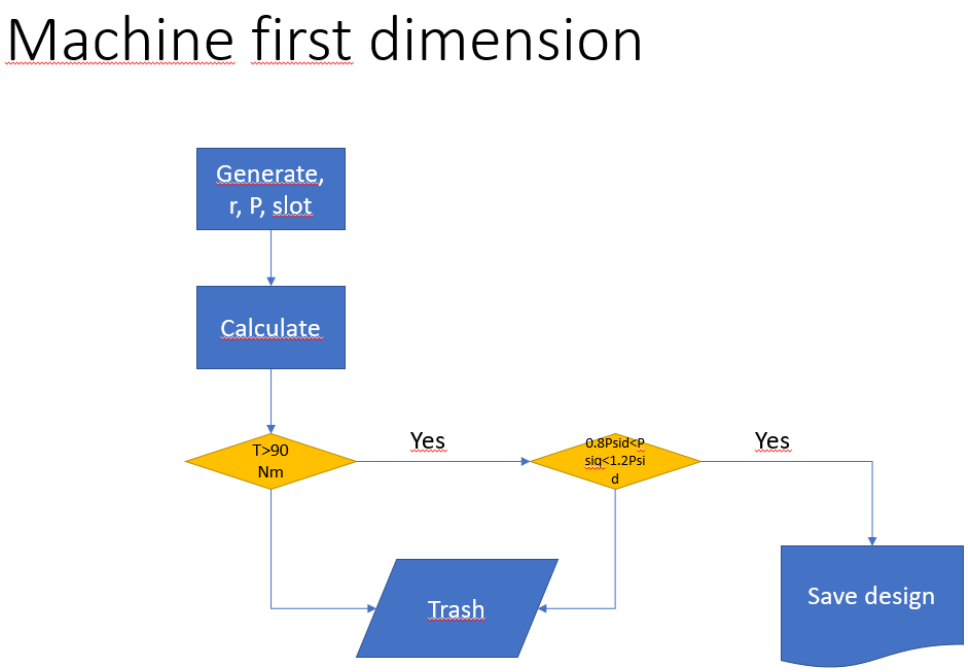


Figure 9. Evaluation process step 1.

Further analysis of the data shows the best results for Pole pair number 5 and 6, and the radius should between160-200 mm. So, a new analysis is made with the following data input:

ry = 160... 200 mm
p=5 or 6
Slot width 10.. 20 mm
Slot depth 12.. 22 mm
Magnet thickness 2..5 mm

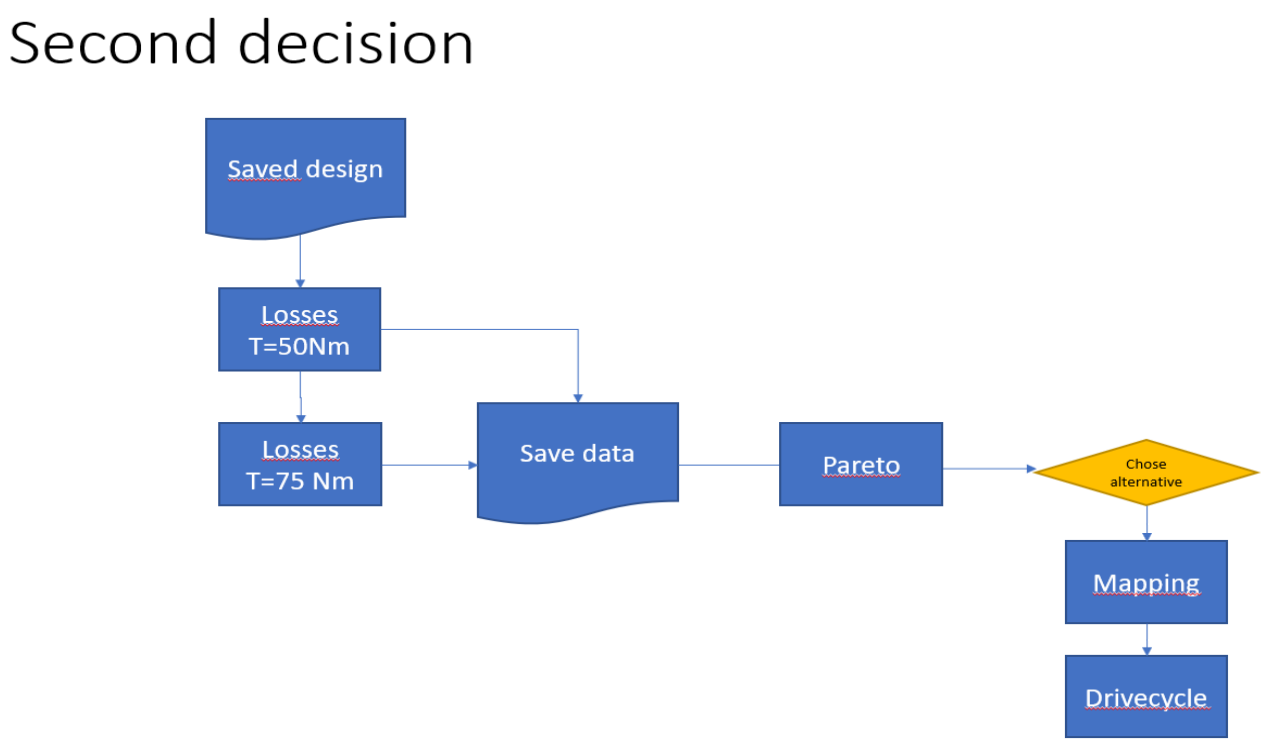


Figure 10. Evaluation process step2.

From the second calculation, and speed 2500 rpm, we get the weight-loss plots according to Figure 11. Each star represents a unique combination of parameters, and the resulting losses can be evaluated towards the weight. Here one could use some sort of cost function.

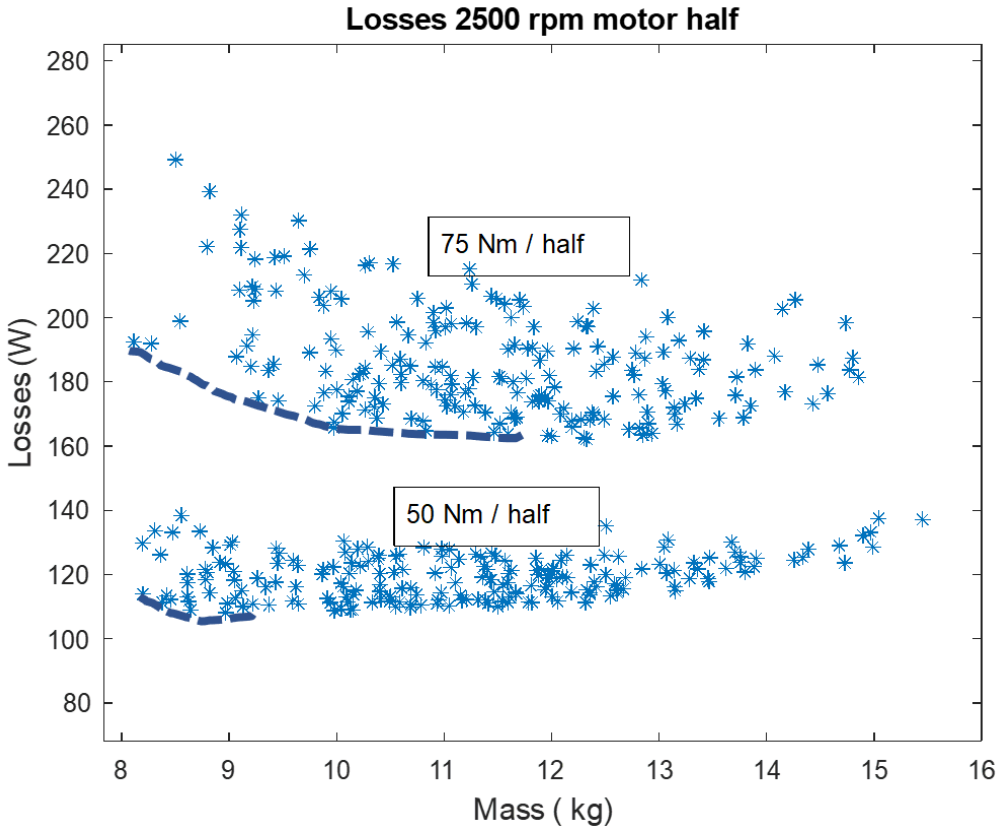


Figure 11. Results from calculations on 2500 rpm and two different torques.

The lowest losses at 75 Nm can be found around 12 kg but for 50 Nm the optimal weight is around 9 kg.

This method worked for a while, and the conclusions from the above results was used further on in the calculations. The program started to become less stable and the mission of evaluating thousands of construction variants was omitted. The value of this type of investigation is also limited when the speed and torque is fixed. The overall drive cycle must be considered, and it would be very interesting to do this type of calculations based on a whole map of data. The computer time would increase with approximately 250 times, but there might be methods to minimize data points and hence the computer time.

The weight of 11-12 kg is chosen, and the machines with lowest losses have the slot width around 17 mm and the radius is 160-180 mm. For further optimisation, the whole torque/speed and operating region of the machines were used, and smaller alterations was made to increase torque, field weakening or decrease the losses. The work was done using trial and error combined with some tens of years of machine evaluation experience. In some cases, the air gap is also adjusted to increase the armature reaction. The minimum air gap is 0.7 mm, which is considered as reasonable. The machines are progressively developed from #1 to #5, and then a comparison with another machine type is done in machine #6.

**Machine #1**

The mean data of the 20 machines with lowest losses at 2500 rpm and 75 Nm are used as input. Data are shown in Table 15.

Table 15. Main data of machine #1 whole machine

| | |
|---|---|
| Outer diameter | 360 mm |
| Inner diameter | 252 mm |
| Air gap | 1 mm (per side) |
| Number of poles | 10 |
| Number of slots | 15 |
| Stator length | 32 mm |
| Rotor length | 19.5 mm |
| Core material | NO30 |
| Voltage | 365 V |
| Phase Current | 187.4 |

Table 16. Slot data

| | |
|---|---|
| b0 | 3 mm |
| b1 | 20 mm |
| b2 | 20 mm |
| hs0 | 1 mm |
| hs1 | 1 mm |
| hs2 | 14 mm |

Table 17. Winding and magnet data

| | |
|---|---|
| Magnet thickness | 3.3 mm |
| Magnet width | 85 % of pole |
| Magnet material | NMX-37 |
| Magnet temp | 100 °C |
| Number of turns | 20 per slot |
| Fill factor | 53,00% |
| Turn length | 198 mm |
| Copper diameter | 3.1 mm |
| No. parallell con | 2 |
| $R_s$ ( Maxwell) | 40 mΩ |
| Mcu | 4.67 kg |
| Mstator | 9.00 kg |
| Mnd | 2.16 kg |
| Mrotor | 12.80 kg |
| Jcu @ 240 Nm | 12.4 A/mm2 |

The efficiency map of machine #1 is shown in Figure 12. Obviously, the machine is not so good at high speed and it is not able to produce the desired torque. The inductance of the machine is too low which results in that most of the current is used for field weakening at high speed.

The turn length of the machine is calculated from the pole pitch and a coefficient that is used in RMxPRT. The concentrated end winding is 115 % of the pole pitch.

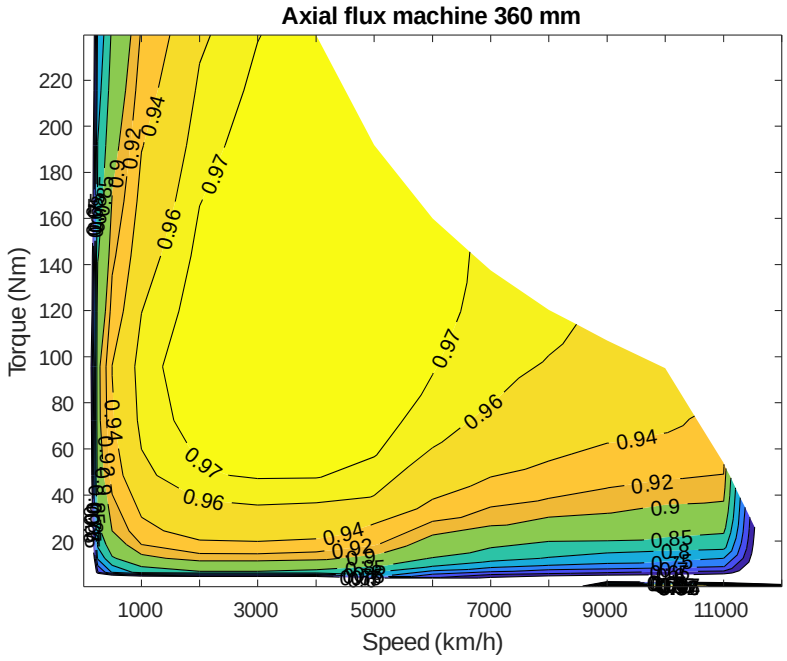


Figure 12. Efficiency map of Machine#1

**Machine #2**

To increase the high-speed torque, the current loading is increased using a smaller outer diameter and length which means lower flux, and a slightly smaller slot area, hence higher current density, and slightly lower fill factor. The winding inductance is increased by means of shorter air gap and magnet thickness. The copper diameter is reduced, resulting in a longer winding turn length, although, the resistance is lower than in Machine #1 due to the smaller slot area. The total weight is substantially reduced.

Table 18. Main data of machine #2

| | |
|---|---|
| Outer diameter | 320 mm |
| Inner diameter | 252 mm |
| Air gap | 0.7 mm (per side) |
| Number of poles | 10 |
| Number of slots | 15 |
| Stator length | 32 mm |
| Rotor length | 13 mm |
| Core material | NO30 |
| Voltage | 365 V |
| Phase current | 193 A |

Table 19. Slot data

| | |
|---|---|
| b0 | 3 mm |
| b1 | 17.8 mm |
| b2 | 17.8 mm |
| hs0 | 1 mm |
| hs1 | 1 mm |
| hs2/half | 12.4 mm |

Table 20. Winding and magnet data

| | |
|---|---|
| Magnet thickness | 2.9 mm |
| Magnet width | 85 % of pole |
| Magnet material | NMX-37 |
| Magnet temp | 100 °C |
| Number of turns | 20 per slot |
| Fill factor | 52,60% |
| Turn length | 223 mm |
| Copper diameter | 2.8 mm |
| No. parallell con | 2 |
| $R_s$ ( Maxwell) | 35.7 mΩ |
| mcu | 3.30 kg |
| mstator | 6.42 kg |
| mnd | 1.50 kg |
| mrotor | 6.36 kg |
| Jcu | 13.7 A/mm2 |

The efficiency map of Machine #2 is shown in Figure 13.

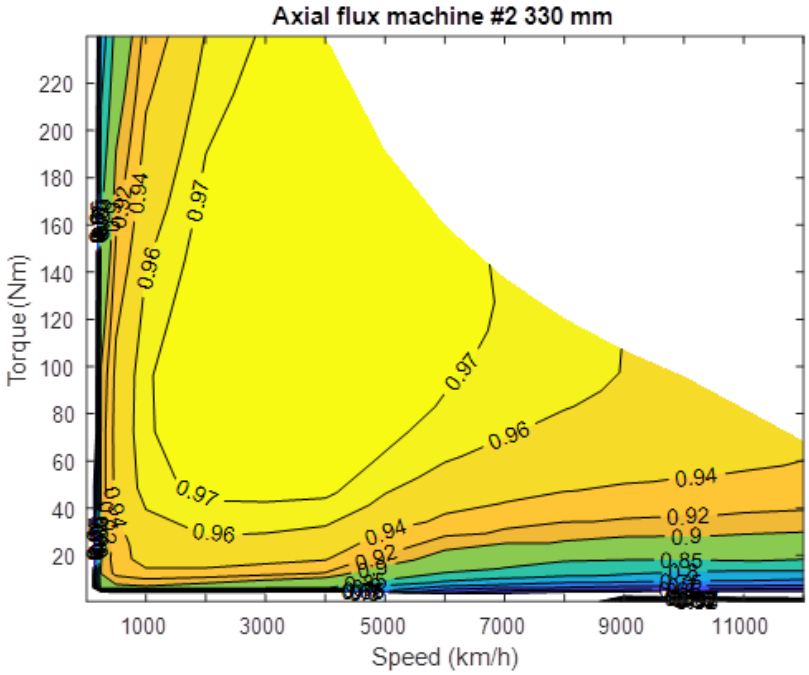

Figure 13. Machine #2 but without rotor losses.

The second machine has better high-speed performance but the losses at high speed are still higher than in the comparable reference motor. The machine has no reluctance torque, so the current needed for field weakening doesn't produce any torque. Of that reason, this rotor type is abandoned in favour of the alternative rotor.

## *5.4 Axial flux machine with alternative rotor*

The construction with concentrated windings and surface mounted magnets produces a lot of losses unless the magnets are divided in small pieces.

To address this problem, inset magnets are used and most often a variant of V-shaped magnets as in Figure 4 are deployed. This allows waves introduced by the winding to circulate in the core between the air gap and the magnet and it also introduces a reluctance torque that is used during field weakening.

A V-shaped magnet may be introduced also in axial flux machines, but the shape can be hard to manufacture in the rotor core, so a simplified inset magnet is tested. The inset magnet-type is often used but the performance is not so good as the V-shaped magnet. In radial flux machines it was used early in the first Prius-machine. See Figure 14.

Figure 14. Inset magnet Prius machine

At the corner of the magnet, a bridge made of the lamination is holding the rotor together when the centrifugal forces act on the magnet. This bridge also works as a leakage path for the magnet flux why there is a need for minimising the thickness of the bridge.

In the axial flux machine, the bridge could be placed in the corresponding position but there is no need for counteracting the centrifugal forces, which will act in the radial direction. There is a need for holding the magnet in place axially, but this can be made with other solutions such as glue, so the bridges are omitted. A pole shoe made of iron powder Somaloy is mounted on the magnet. The construction will shelter off some of the flux that otherwise would go into the magnet and in that way rotor losses are lowered and comparable to the radial flux machine.

The soft magnetic part placed in between the magnets will also serve as a concentrator for flux in the q-direction, which will result in a reluctance torque which is useful at high-speed operation.

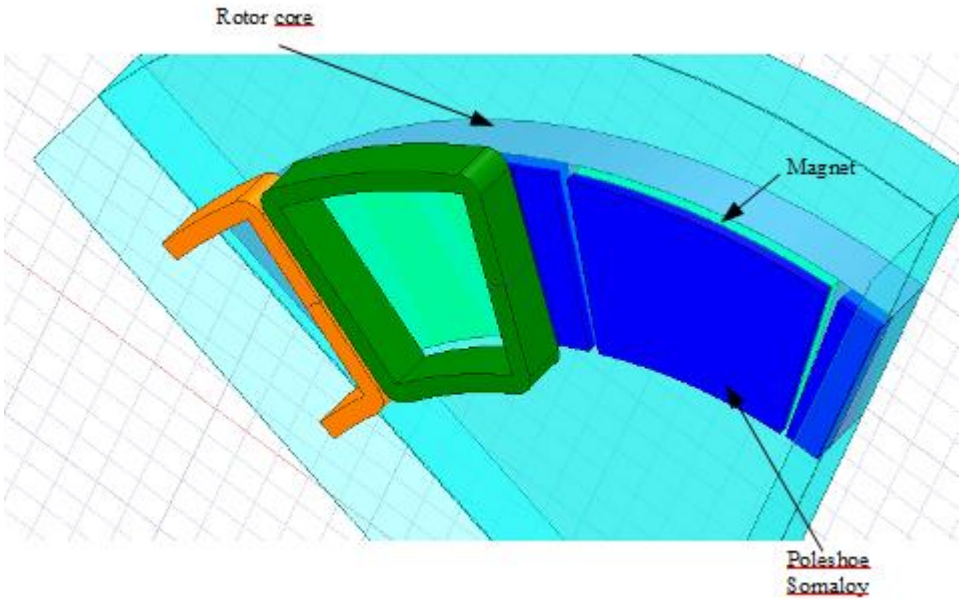


Figure 15. Axial flux inset magnet

The cross section of the pole is shown in Figure 16.

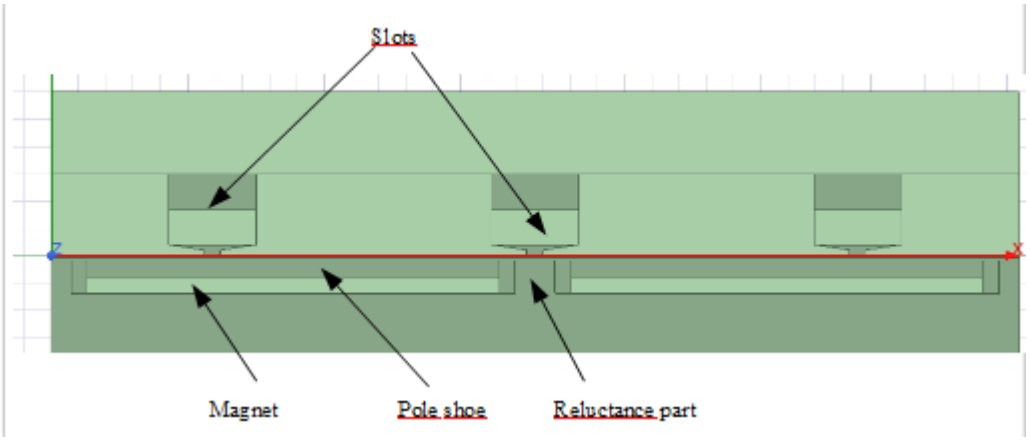


Figure 16. Cross section of inset magnets.

With the surface mounted magnet, the induced currents produce a lot of losses unless the magnets are divided. It is found in [4] that the surface mounted magnet must be divided in 18 pieces, to have reasonable rotor losses. The rotor losses of the inset magnet and a pole shoe are approximately 3800 W at 6000 rpm which is also rather high, and the inset magnet must also be divided. An estimation is that at least 8 pieces per magnet is needed.

**Machine #3 Concentrated winding**

Table 21. Main data of machine #3

| | |
|---|---|
| Outer diameter | 310 mm |
| Inner diameter | 217 mm |
| Air gap | 0.9mm (per side) |
| Number of poles | 10 |
| Number of slots | 15 |
| Stator length | 30 mm |
| Rotor length | 29.9 mm |
| Core material | NO30 |
| Rotor material | Somaloy 1000 |
| Voltage | 365 V |
| Phase current | 213.5 |

Table 22. Slot data

| | |
|---|---|
| b0 | 3 mm |
| b1 | 16 mm |
| b2 | 16 mm |
| hs0 | 1 mm |
| hs1 | 1 mm |
| hs2 | 13 mm |

Table 23. Winding and magnet data, weights are per half

| | |
|---|---|
| Magnet thickness | 3.4 mm |
| Magnet width | 70 % of pole |
| Magnet material | NMX-37 |
| Magnet temp | 100 °C |
| Number of turns | 22 per slot |
| Fill factor | 52,60% |
| Turn length | 192 mm |
| Copper diameter | 2.6 mm |
| No. parallell con | 1 |
| $R_s$ | 49.7 mΩ/half |

| | |
|---|---|
| Mcu | 3.00 kg |
| Mstator | 6.44 kg |
| Mnd | 1.36 kg |
| Mrotor | 15.38 kg |
| Jcu | 20.3 A/mm2 |
| Pole shoe height | 7 mm |

The efficiency of the third machine without the magnet losses are shown in Figure 17 and in Figure 18 the magnet losses are added when the magnets are divided in eight pieces. It doesn't influence the normal operating area so much but at high speed and high torque the losses create a thermal problem.

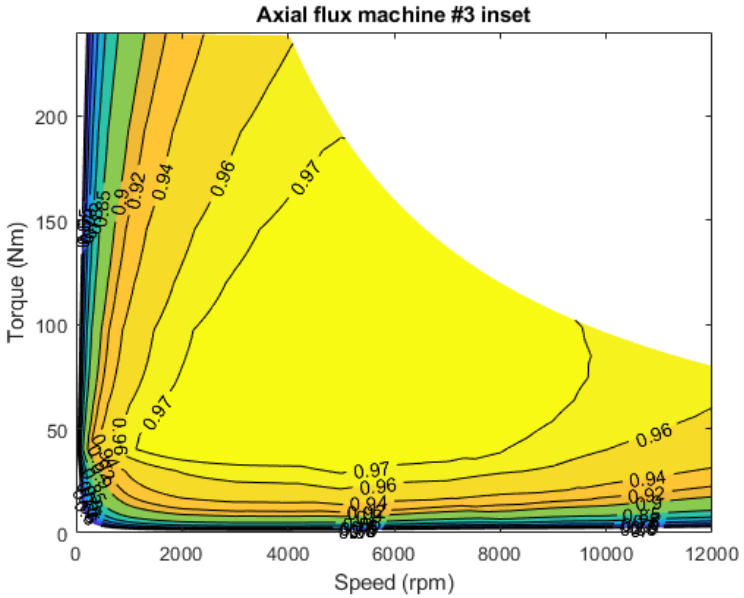


Figure 17. Machine #3 without rotor losses.

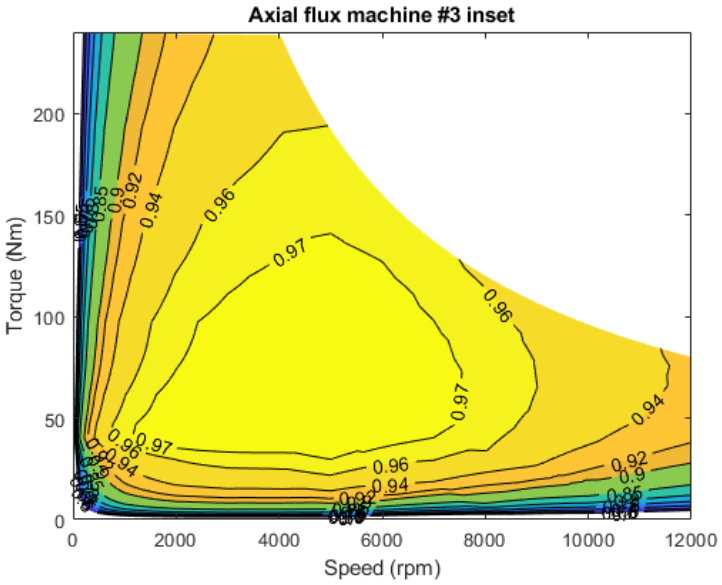


Figure 18. Machine #3 with rotor losses into account. Each magnet is divided in eight pieces.

In order to further decrease the rotor losses, a machine with distributed windings is analysed.

**Machine #4, distributed winding**

The winding type is changed from the concentrated winding to a distributed one. The simplest version is used with three slots per pole. Main data remains the same, and the material weight is similar, except for the copper weight which is 58% more than for Machine #3 (with concentrated windings).

Table 24. Main data of machine #4

| | |
|---|---|
| Outer diameter | 310 mm |
| Inner diameter | 217 mm |
| Air gap | 0.9mm (per side) |
| Number of poles | 10 |
| Number of slots | 30 |
| Stator length | 30 mm |
| Rotor length | 29.9 mm |
| Core material | NO30 |
| Rotor material | Somaloy 1000 |

Table 25. Slot data

| | |
|---|---|
| b0 | 3 mm |
| b1 | 8 mm |
| b2 | 8 mm |
| hs0 | 1 mm |
| hs1 | 1 mm |
| hs2 | 13 mm |

Table 26. Winding and magnet data,

| | |
|---|---|
| Magnet thickness | 3.4 mm |
| Magnet width | 70 % of pole |
| Magnet material | NMX-37 |
| Magnet temp | 100 °C |
| Number of turns | 10 per slot |

| | |
|---|---|
| Fill factor | 52,60% |
| Turn length | 297.3 mm |
| Copper diameter | 2.8 mm |
| No. parallell con | 1 |
| $R_s$ ( Maxwell) | 52.1mΩ/half |
| Mcu | 4.75kg |
| Mstator | 6.39 kg |
| Mnd | 1.36 kg |
| Mrotor | 15.3 kg |
| Jcu | 20.5A/mm2 |
| Pole shoe height | 7 mm |

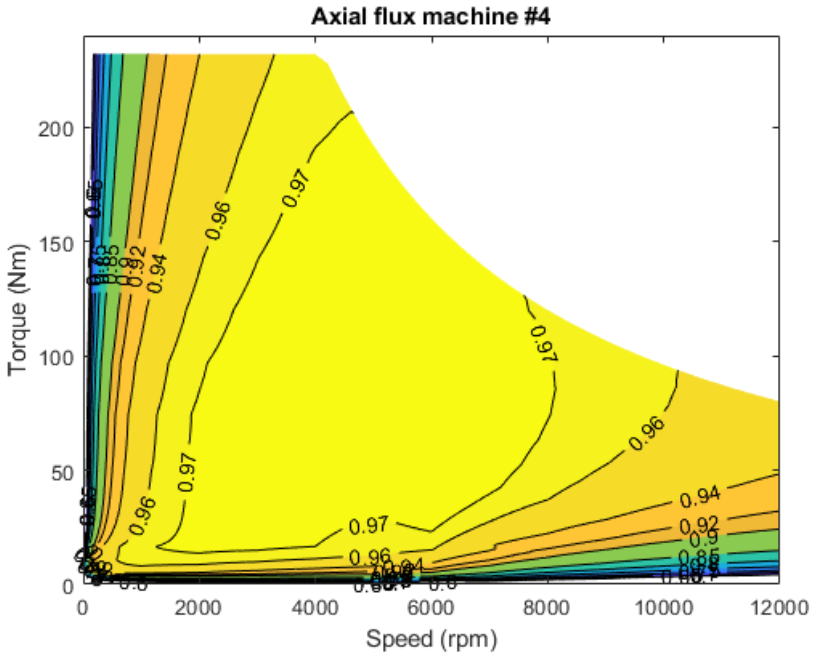


Figure 19. Efficiency of Machine #4 with distributed winding

With the distributed winding and the magnet cut in half radially, the magnet losses are 112 W at 240 Nm and 4000 rpm, which is considered as good.

## *5.5 Axial flux machine with grain-oriented material*

Grain-oriented magnetic material is mostly used in transformers, Gunther et.al. [8]. The material is developed towards low losses at 50 or 60 Hz. It's important in the grain-oriented material to get the magnetic orientation in the right direction and different methods are used to improve this property. Other important features are the losses and permeability as well as the magnetostriction levels that can produce noise. A lot of efforts are made to lower the energy loss during production and on making low-cost production processes.

With the axial flux machine and central stator, there is an opportunity for using grade-oriented laminations. The development of this material is progressing towards really low losses. We have gathered data from Sura and Thyssen Krupps but the information on losses at different frequencies are hard to find.

The data used are 'invented' in that way that the losses are scaled from 50 Hz to higher frequency according to the data in [9], which is reporting on a non-oriented lamination with losses around 1 W/kg at 1.0 T. Gunther et.al., [8] predicts losses lower than 0.8 W/kg at 1.7 T for grain-oriented laminations which is very low compared to ordinary laminations used in electric motors.

Thyssen-Krupp have several different types, some above and some under 1 W/kg @1.7T, 50 Hz. Based on the information above, a fictive material with 1 W/kg at 1.7T, 50 Hz, and frequency behaviour from different sources, have been created. Most commercial material are made for 50/60 Hz so of that reason the thickness normally isn't lower than 0.3 mm. A special material made for axial flux high speed machines could have thinner laminations and the eddy current losses could be lower than in the material described in Figure 20 and 21. Anyway, the losses at 50 Hz is lower compared to ordinary isotropic (non-oriented) laminations which typically have 2.5 W/kg @1.5T, 50 Hz, so there is a potential to produce low loss machines.

.

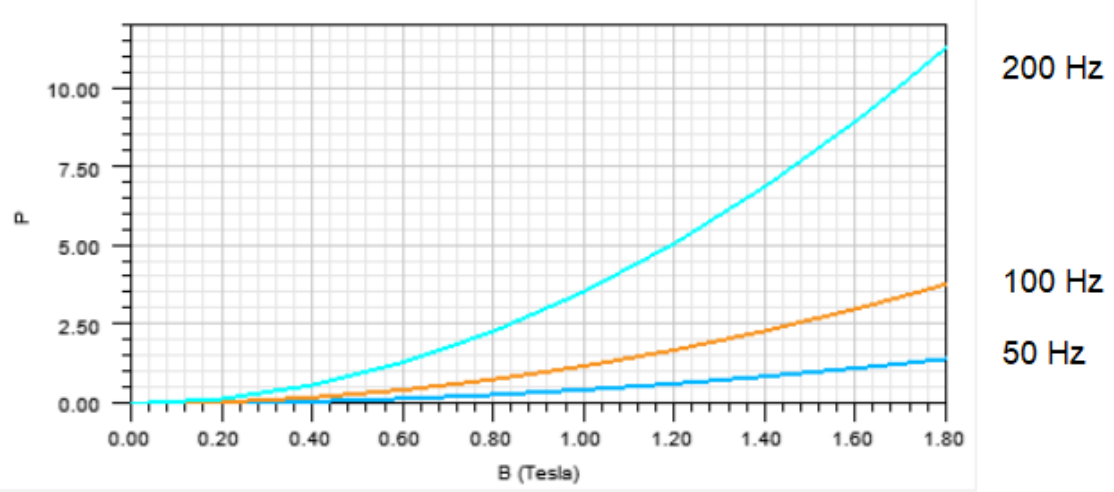


*Figure 20 Losses of 'invented' grain-oriented material*

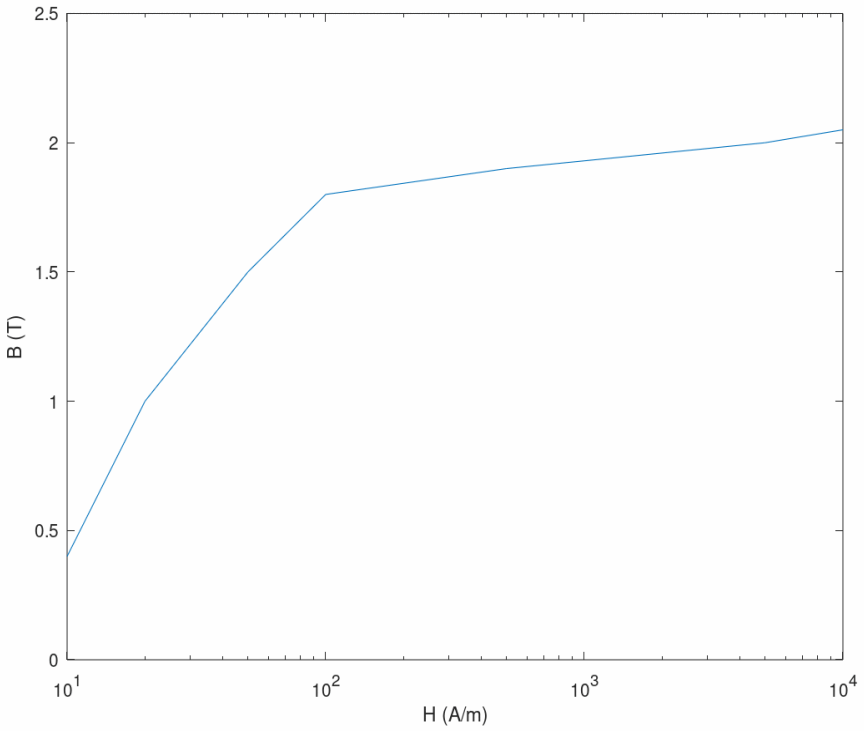


*Figure 21. BH-curve of the grain-oriented material.*

**The Machine #5** has laminations in the teeth made of the grain-oriented material. The efficiency is better at low speed and low torque.

As a start the same measures are used in this machine as in the machine #4 but an attempt to lower the losses at high speed was done. Using shorter air gap and thinner magnet wasn't successful and the conclusion is that the eddy current losses of the core dominate at high speed. In Figure 22, it is shown that the efficiency is improved at low speed and low torque. The rotor length is slightly increased in order to improve the flux and at the same time the magnet is shorter. Combined with lower air gap a machine is calculated.

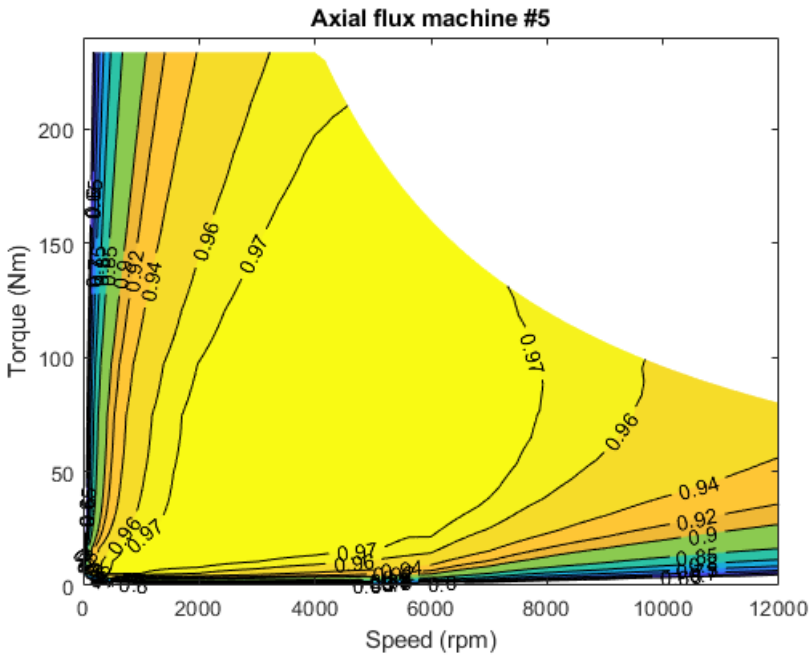


*Figure 22. Efficiency of machine #5.*

The different losses are shown Figures 23 and both the copper and iron core losses are high at high speed.

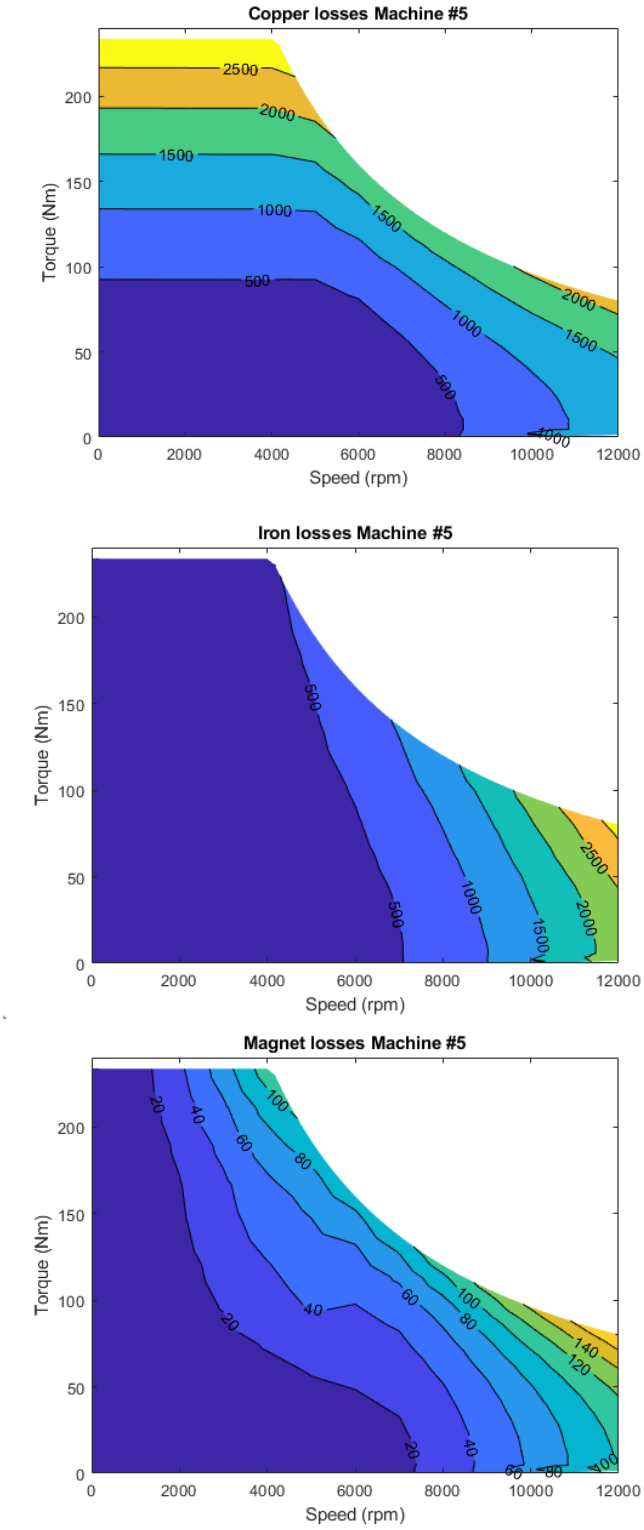


*Figure.23 a) Copper losses b) Iron losses c) Losses in solid magnets*

Table 27. Main data of machine #5

| | |
|---|---|
| Outer diameter | 310 mm |
| Inner diameter | 217mm |
| Air gap | 0.8mm (per side) |
| Number of poles | 10 |
| Number of slots | 30 |
| Rotor length | 30.9 mm |
| Core material | GO-mtrl |
| Rotor material | Somaloy 1000 |
| Voltage | 299 V |
| Phase Current | 234.6 A |

Table 28. Slot data

| | |
|---|---|
| b0 | 3 mm |
| b1 | 8.0 mm |
| b2 | 8.0 mm |
| hs0 | 1 mm |
| hs1 | 1 mm |
| hs2/half | 13. mm |

Table 29. Winding and magnet data

| | |
|---|---|
| Magnet thickness | 2.9 mm |
| Magnet width | 70 % of pole |
| Magnet material | NMX-37 |
| Magnet temp | 100 °C |
| Number of turns | 9 per slot |
| Fill factor | 52,60% |
| Turn length | 311.3 mm |
| Copper diameter | 3.14 mm |
| No. parallell con | 1 |
| $R_s$ | 42.2 mΩ/half |
| Mcu | 4.40 kg |
| Mstator | 7.82 kg |
| Mnd | 1.16 kg |

| | |
|---|---|
| Mrotor | 18.3 kg |
| Jcu | 21.8 A/mm2 |
| Pole shoe | 7.0 mm |

## *5.6 Axial flux machine with toroidal winding*

The axial flux machine with toroidal winding has shorter end windings compared to the distributed winding. The drawback is that a back iron core is necessary in the central stator of the machine for closing the flux. The machine has a radial flux equivalent that is a subject for a patent some 30 years ago (if my memory works OK and no investigation on patents have been done).

The toroidal winding has been investigated in [12], where it is found that the phase resistance is much lower in the toroidal winding. In Figure 24, a cross-sectional view of the stator looked upon from the outer radius is shown. In a) the winding is the former distributed winding and in b) we have the toroidal winding. The coils are closed in the axial direction which makes the end winding of the coil shorter.

Using grain-oriented material in this core could work, but in that case the anisotropic data of the grain-oriented material has to be taken into account, which could be a matter for further investigations.

**Machine #6**

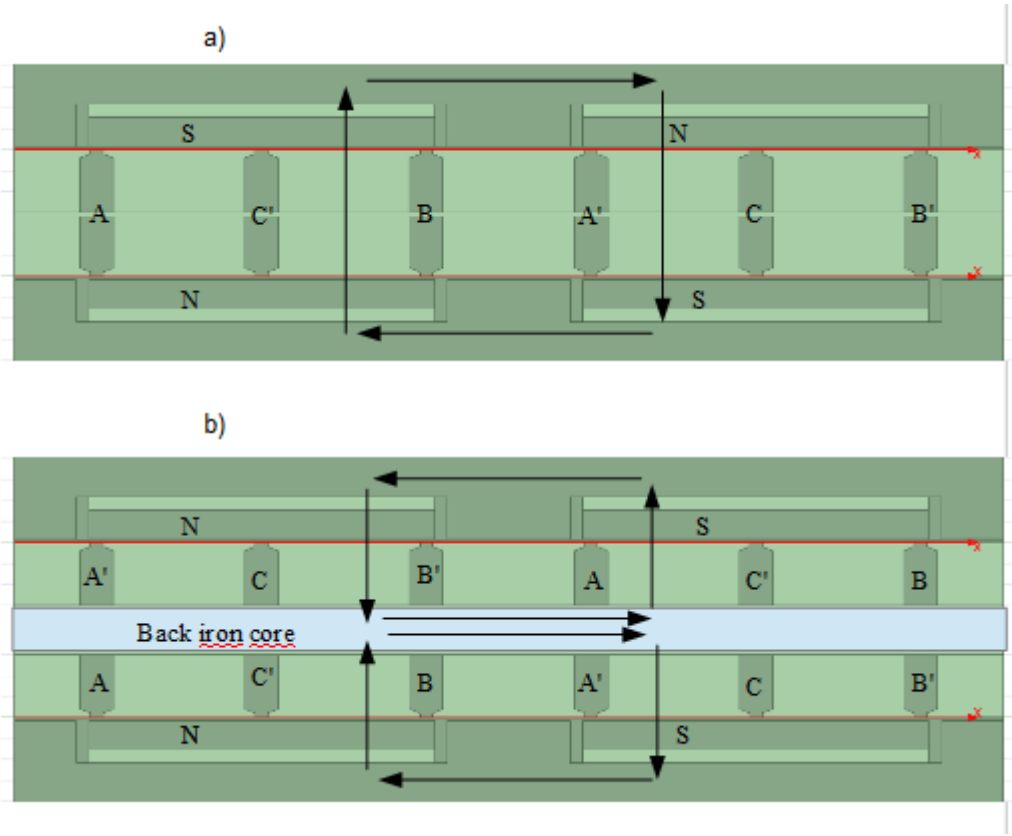


Figure 24. a) Distributed winding. b) Toroidal winding

Machine # 6 have smaller dimensions than the machine number five but with the addition of a core for closing the flux. The core thickness is 24.4 mm, and the stator core weight is increased with 15.7 kg (twice the weight of Machine #5 with the distributed winding), which isn't a low value. The copper weight is however lower which is good as copper is a scares material.

Table 30. Main data of machine #6

| | |
|---|---|
| Outer diameter | 294 mm |
| Inner diameter | 206mm |
| Air gap | 0.8mm (per side) |
| Number of poles | 10 |
| Number of slots | 30 |
| Stator length | 32 mm |
| Rotor length | 30.9 mm |
| Core material | NO30 |
| Rotor material | Somaloy 1000 |
| Voltage | 299 V |
| Phase Current | 269.4 A |

Table 31. Slot data

| | |
|---|---|
| b0 | 3 mm |
| b1 | 7.0 mm |
| b2 | 7.0 mm |
| hs0 | 1 mm |
| hs1 | 1 mm |
| hs2/half | 11. mm |

Table 32. Winding and magnet data

| | |
|---|---|
| Magnet thickness | 2.9 mm |
| Magnet width | 70 % of pole |
| Magnet material | NMX-37 |
| Magnet temp | 100 °C |
| Number of turns | 10 per slot |
| Fill factor | 52,60% |

| | |
|---|---|
| Turn length | 104.8 mm |
| Copper diameter | 3.2 mm |
| No. parallell con | 1 |
| $R_s$ | 15.8 mΩ/half |
| Mcu | 0.95 kg |
| Mteeth | 14.8 kg |
| Mcore | 8.7 kg |
| Mnd | 1.08 kg |
| Mrotor | 14.3 kg |
| Jcu | 27.1 A/mm2 |
| Pole shoe | 4.0 mm |

The efficiency of the machine is shown in Figure 25. The machine has to be redesigned in some way, the peak torque is too low, and the high-speed torque is too weak. Some problems also disturbed the finalisation with frequent breaks of execution.

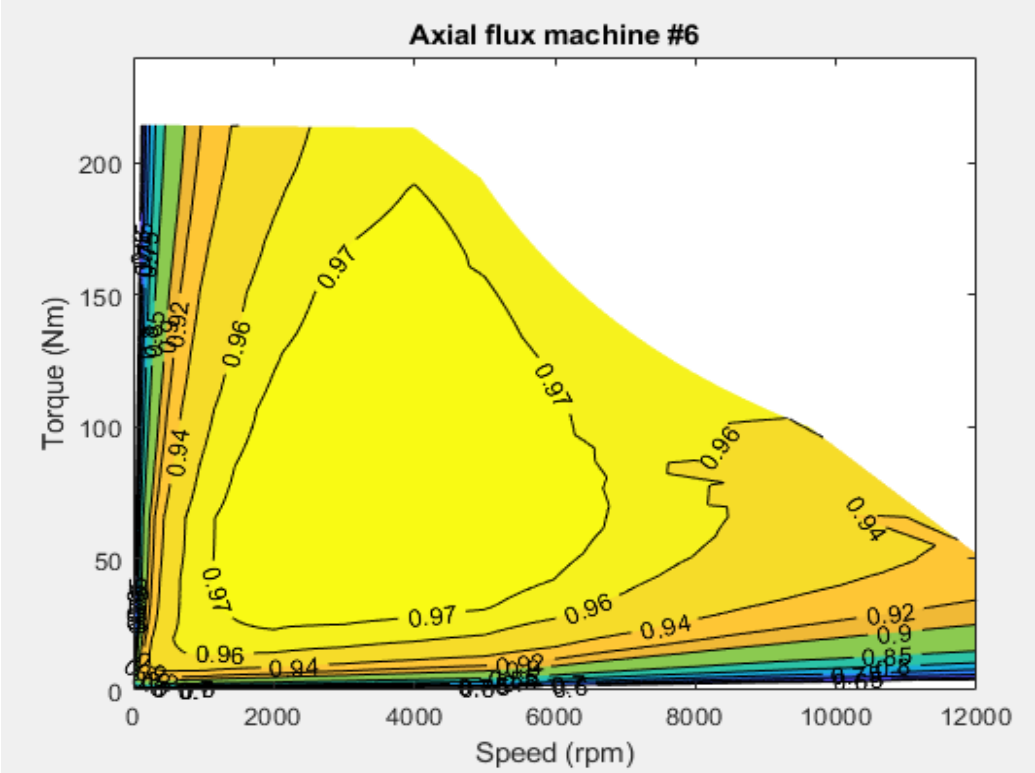


Figure 25. *Efficiency of machine #6.*

# 6. Results from drive cycle evaluations and comparison to 3D

## *6.1 Drive Cycles*

The energy used is calculated over the distance, as well as the loss. Only the losses of the motor are investigated. The two last evaluations with constant acceleration and retardation and hills are done 10 times. The losses are presented in kWh / 100km, which is the standard notation for cars in the EU. See also a summary of the different designs and efficiency maps in Appendix D.

Table 33. Energy losses kWh/100km when geared for 140 km/h

| kWh/100 km | Ref Motor | #1 | #2 | #3 | #4 | #5 | #6 |
|---|---|---|---|---|---|---|---|
| | v-PM, distr. wind. RFM | surface PM | smaller than #1, higher J | inset PM conc. wind. | inset PM distr. wind. | GO core | toroidal wind. |
| WLTP | 1.191 | - | 2.090 | 1.293 | 1.334 | 1.114 | 1.286 |
| US06 | 1.524 | - | 2.739 | 1.576 | 2.046 | 1.235 | 1.804 |
| Hills 8% | 2.003 | - | 3.166 | 2.074 | 2.823 | 2.474 | 2.850 |
| 120 km/h | 1.534 | - | 3.192 | 1.987 | 2.514 | 2.168 | 2.134 |

Overall, the axial flux machines have higher losses compared to the radial flux machine. Machines #1 - 3 assumes very fine divided magnets and may be impossible to realise and the high-speed data of machine # 1 isn't good enough. The second machine has better high-speed torque but the losses at high speed is too high. The machine #3-5 have inset magnets and better high-speed performance. The machine #5 with grain oriented (GO) laminations has good performance for the low-speed cycles and is comparable to the reference machine. At higher speed, the result is not so good, and, in those cases, the radial flux machine is superior.

The machine #6 with another toroidal configuration seems to work quite well. The time to investigate this machine type was short and it could be interesting to work on this machine type. It solves some problems, but the increased core losses and the increased weight are not so good.

The weight of active material of the machines are summarised in Table 34.

Table 34. Weight of active material

| Weight/kg | Ref Motor | #1 | #2 | #3 | #4 | #5 | #6 |
|---|---|---|---|---|---|---|---|
| Magnet | 1,25 | - | 1,5 | 1,4 | 1,4 | 1,2 | 1,1 |
| Total | 25,3 | | 17,6 | 26,2 | 27,8 | 31,7 | 39,8 |

One benefit with the axial flux machine is the low weight but this is only valid for the surface

mounted machine #2. When moving to inset magnets, the weight increase and is almost the same as for the radial flux machine. The best axial flux machine #5 have higher weight than the radial flux machine but one could consider surface mounted magnets and distributed winding as an alternative. The last machine #6 doesn't actually perform well enough, with lower efficiency and higher weight than the radial flux machine.

## *6.2 Comparison to 3D*

The 2D simulations of machine #3, with inset permanent magnets and concentrated windings, is verified in three points with 3D-simulations.

Table 35. 2D-calculated values of machine #3.

| Speed rpm / Torque Nm | 2D Torque( Nm) | 2D Cu losses | 2D Core losses | 2D Magnet losses |
|---|---|---|---|---|
| 4000/240 | 239,8 | 3538 | 811 | 896 |
| 4000/120 | 119,8 | 772 | 454 | 183 |
| 8000/160 | 159,8 | 2131 | 1845 | 2280 |

Table 36. 3D-calculated values of machine #3.

| Speed rpm / Torque Nm | *4000/240* | | | *4000/120* | | | *8000/160* | | |
|---|---|---|---|---|---|---|---|---|---|
| | *2D* | *3D* | *difference* | *2D* | *3D* | *difference* | *2D* | *3D* | *difference* |
| Torque ( Nm ) | 239,8 | 225 | 7% | 119,8 | 120,6 | -1% | 159,8 | 121,6 | 31% |
| Pcu (W) | 3538 | 2101 | 68% | 772 | 816 | -5% | 2131 | 1605 | 33% |
| Pcore (W) | 811 | 673 | 21% | 454 | 417 | 9% | 1845 | 2716 | -32% |
| Pmagnet (W) | 896 | 2164 | -59% | 183 | 472 | -61% | 2280 | 6220 | -63% |

The 2D simulation results compare rather well with the 3D simulation results, at least for the mid-speed/mid-torque operating point (4000 rpm/120 Nm), with the exception for the magnet loss. The copper losses calculated in 3D are lower in two cases but higher in one. The value given from Rmxprt coincides with the 2D-values rather well, but the 3D-values deviate.

Likewise, the 2D simulations of machine #5, with inset permanent magnets, distributed windings and grain-oriented stator core, is verified in three points with 3D-simulations.

Table 37. The machine #5 with distributed winding with a solid magnet

| Speed rpm / Torque Nm | 2D Torque(Nm) | 2D Cu losses | 2D Core losses | 2D Magnet losses |
|---|---|---|---|---|

| | | | | |
|---|---|---|---|---|
| 4000/240 | 224,2 | 2890 | 756 | 112 |
| 4000/120 | 116,6 | 786 | 496 | 39,2 |
| 8000/160 | 123,6 | 1995 | 1657 | 116 |

Table 38. The machine #5 3D calculations

| Speed rpm / Torque Nm | *4000/240* | | | *4000/120* | | | *8000/160* | | |
|---|---|---|---|---|---|---|---|---|---|
| | *2D* | *3D* | *difference* | *2D* | *3D* | *difference* | *2D* | *3D* | *difference* |
| Torque (Nm) | 224,2 | 231 | -3% | 116,6 | 115,1 | 1% | 123,6 | 104 | 19% |
| Pcu (W) | 2890 | 2782 | 4% | 786 | 794 | -1% | 1995 | 1939 | 3% |
| Pcore (W) | 756 | 903 | -16% | 496 | 564 | -12% | 1657 | 1260 | 32% |
| Pmagnet (W) | 112 | 636 | -82% | 39,2 | 547 | -93% | 116 | 880 | -87% |

Again, the 2D simulation results compare rather well with the 3D simulation results, with the exception for the magnet loss. The magnet losses differ a lot in both cases. This time, the error between 2D and 3D is not so high at high speed. The end winding isn't modelled in the 2D-calculation which means that the flux produced by the stator currents is not corresponding to the real case. In the 3D model, the end winding flux is present in both d- and q-direction and it could change the operating point in terms of the d- and q-current. The used current vector has been calculated from the 2D-data and should alter due to the end winding.

The magnet losses calculated in 2D doesn't consider that the current circulates along the ends of the magnet. This circulation path will add resistance to the current and hence affect the magnet losses. A way for estimating these losses is elaborated in [11].

# 7. Rotor core

The rotor core  has been quite thick during the calculations and the rotor stands for a major part of the weight, see Appendix A. Different rotor thickness are investigated on machine #5 at full torque.

The resulting torque is shown in Figure 26 when the rotor thickness, hrotor, is varied but the pole shoe is constant. The thickness of the core may be lowered with one fifth, saving 4 kg in the rotor, but will result in 4 % lower max torque. A shift to a high-grade material instead of Somaloy will also lower the weight due to higher saturation flux density. The saturation flux density can probably be increased from 1.6 to 1.8 T.

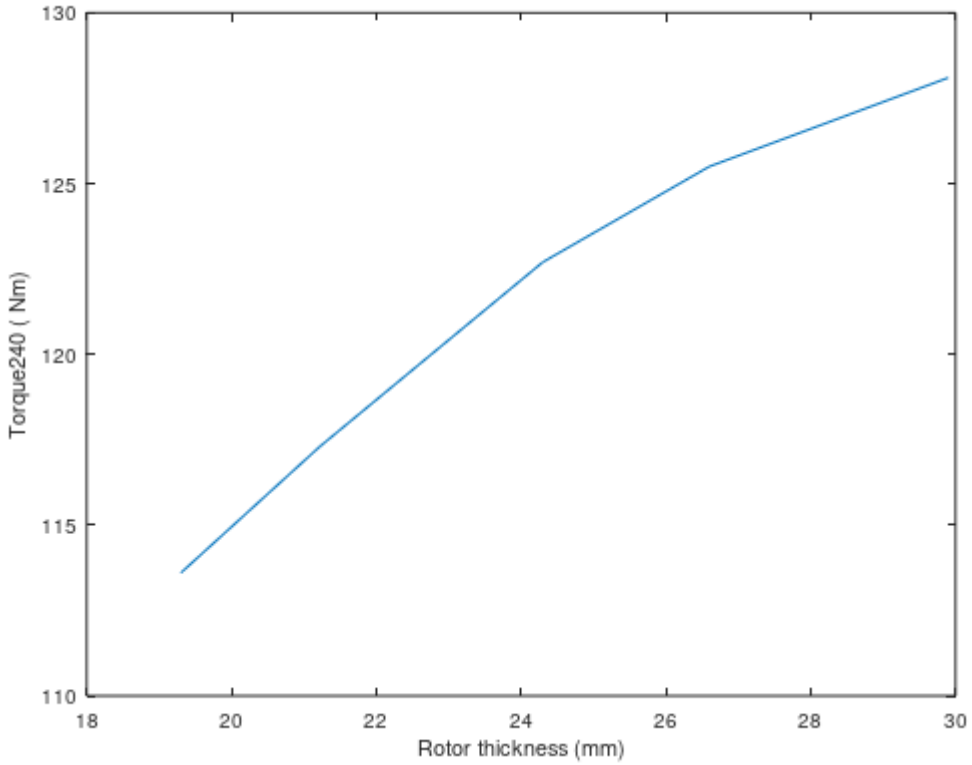


Figure 26 Torque from one section for different rotor thickness.

# 8. Conclusion

The axial flux machine with two rotor discs and a central stator is analysed and compared to a radial flux machine. The comparison is done for different radius of the axial flux machine.

The machines with surface mounted magnets and concentrated windings are not recommended, although they have the lowest weight. They need a high degree of 'laminated' magnets. i.e., the magnets must be divided in small pieces and insulated against each other. If an effective and low-cost producer of these magnets is to be found, the rotor construction is quite simple, and the concentrated winding can have less amount of end winding. If concentrated windings are to be used, this problem must be investigated more thoroughly.

A rotor construction with inset magnets can result in lower magnet losses and the reluctance torque will improve the high-speed performance of this machine. The rotor weight increases due to extra parts in the rotor.

In order to have magnet losses that are acceptable, without dividing the magnet, a distributed winding can be used. The pulsating flux density in the magnet are very much lower with a distributed winding and torque will have lower ripple. The latter could have implications on produced noise from the machine.

The drive cycle calculations show better data for the machines with distributed winding and grain-oriented material compared to the radial flux machine. A core made of grain-oriented material improves mainly the WLTP and US06 cycles due to lower hysteresis losses of the material. However, at higher speed, the reference radial flux machine is better. If it's possible to lower the eddy current losses in the core and in the rotor, it will enhance the performance at high speed. This can be achieved with thinner lamination if the core fill factor can be maintained.

A toroidal winding is beneficial for lowering the copper losses. The core losses and weight of the machine will increase on the other hand.

A method that uses 2D simulations as an approximation of the 3D axial flux machine shows rather good results, as long as the machine isn't in the field weakening region. The simulated loss in the magnet is underestimated in the 2D case.

# 9. Future work

This report suggest that the radial flux machine is in terms of efficiency superior to at least Yasa-type machines. The weight of the radial flux machine is however higher, but this could be reduced with higher speed. The potential in saving material and cost might be higher in this case compared to the axial flux machine. However, increasing gear ratio may result in several gearing steps and should also be considered as well as the influence on the converter. The fundamental frequency of the machine will be higher which influence the performance of the converter

The distributed winding is the one that shows the greatest potential of the studied axial flux machines. The machine with best performance have inset magnets in order to lower the losses but it could be investigated to use surface mounted magnets and distributed winding.

The machines with concentrated winding produce a lot of harmonics on the magnet surface which implies high rotor losses. The concentrated winding is however easy to produce and robust. A segmented magnet could lower the losses and there are producers of magnets that are divided into fine pieces. My experience is that the magnets are expensive but maybe if one big producer of electric vehicles ask them, the price might be low enough, [13].

If concentrated windings or surface mounted magnets are to be used, the rotor losses have to be more thoroughly evaluated. There are big differences between 2D and 3D results and how the mesh density influence the result isn't analysed. At high speed, the current will be concentrated to the outer parts of the magnet and a high mesh density might be necessary. When meshing the machines, I've done very little on investigating the quality of the result. One test of doubling the number of mesh elements resulted in small difference to the original meshing. The time step used varies with speed, and for one electric period I've used 40 steps. The error introduced due to meshing and time steps is regarded as low compared to the error due to 2D, but it can be further investigated.

# References


[1] S. Gair, A. Canova, J. F. Eastham, and T. Betzer, “A new 2D FEM analysis of a disc machine with offset rotor,”in Proc. Int. Conf. Power Electronics, Drives and Energy Systems for Industrial Growth, vol. I, 1995, pp. 617–621

[2] J.F.Gieras and M.Wing,PermanentMagnetMotorTechnology-Design and Applications New York, 1997.

[3] Parviainen A. et.al., 'Modeling of Axial Flux Permanent-Magnet Machines', IEEE TRANSACTIONS ON INDUSTRY APPLICATIONS, VOL. 40, NO. 5, SEPTEMBER/OCTOBER 2004

[4] Alatalo M. , 'Axial flux machine as a traction motor for electric and hybrid vehicles', Technical report 2018:1, Chalmer University of Technology 2018

[5] Alatalo,'Thermal evaluation of a propulsion motor for electric air-craft' , Proc of ICEM2020

[6] Tillman et.al.,'Elmaskiner för fordon i en cirkulär ekonomi', Rapport från FFI-projekt nr 44204-1

[7] https://dieselnet.com/standards/cycles

[8] Gunther K. et.al., 'Recent Technology Developments in the Production of Grain-Oriented Electrical Steel', Steel Research 2005

[9] Mehdi et.al. , 'Non-oriented electrical steel with core losses comparable to grain-oriented electrical steel', *Journal of Magnetism and Magnetic Materials 491 (2019) 165597*

[10] Sundario et.al.,'Effect of Different Cutting Techniques on Magnetic Properties of Grain Oriented Steel Sheets and Axial Flux Machines' *2019 IEEE*

[11] Tidblad , Roshanfekr,'Two-Dimensional and Three-Dimensional Core and Magnet Loss Modeling in a Radial Flux and a Transverse Flux PM Traction Motor', IEEE TRANSACTIONS ON INDUSTRY APPLICATIONS, 2017

[12] Kim et.al.,'Closed-Form Solution for Axial Flux Permanent-Magnet Machines With a Traction Application Study', IEEE TRANSACTIONS ON INDUSTRY APPLICATIONS, 2016

[13] https://www.arnoldmagnetics.com/products/l-type-laminated-magnets/

[14] Alatalo.M., 'Efficiency impact of motor type and motor size choice', Technical report 2021:1, Chalmer University of Technology 2021

# Appendix A. Slot and rotor pole

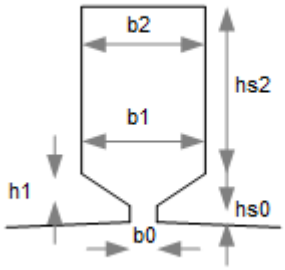


Figure A1. Slot dimensions

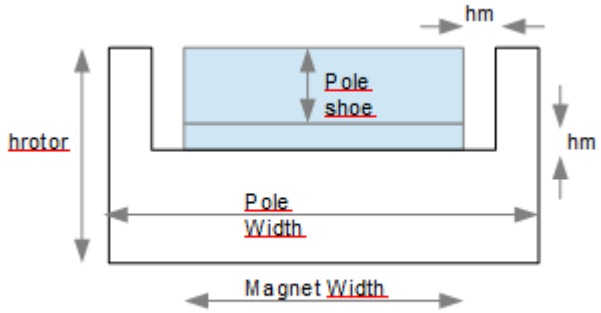


Figure A2. Rotor dimensions

## *Appendix A.1 Rotor of concentrated winding*

A smaller alteration of the rotor model of the concentrated winding is done. The magnet is divided in two pieces which is done to lower the eddy currents in the magnet. The magnet pieces are separated 1 mm.

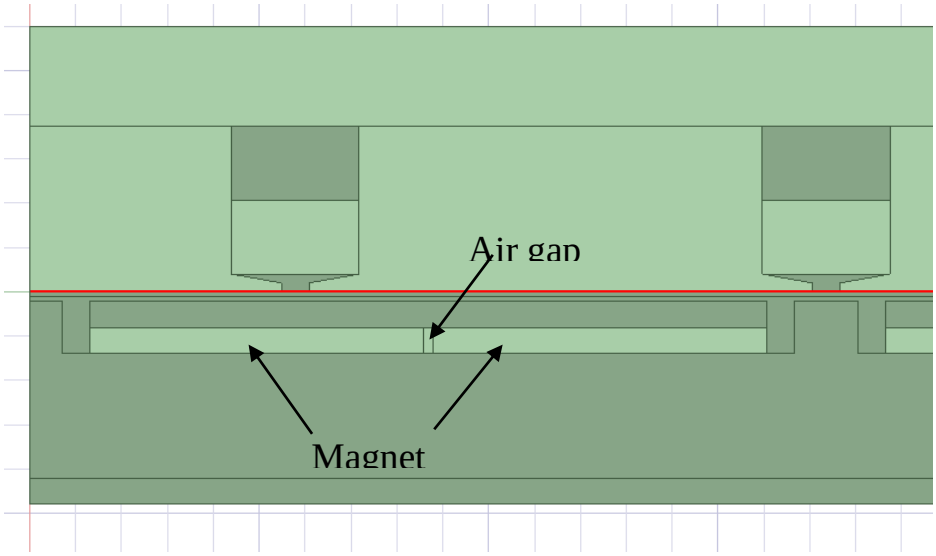


Figure A.3. Concentrated winding rotor

# Appendix B. Programs that are used.

A machine, when found a good compromise on slot dimensions and radius, is analysed in three steps, see Figure B1.

Guessing a suitable number of turns in the winding and current level, the first step is to calculate the flux of the machine for different current levels in d-direction and q-direction.

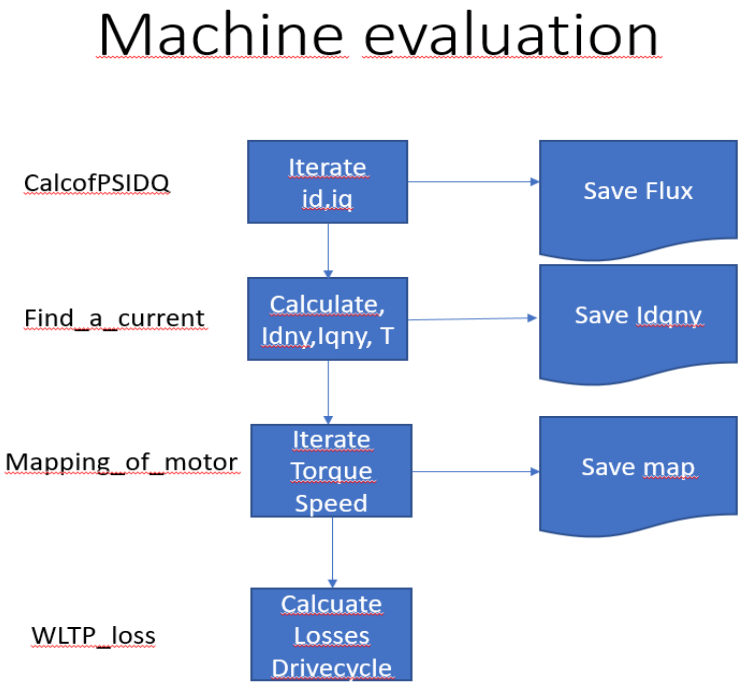


Figure B1. Evaluation process

The resulting flux could look like in Figure B2.

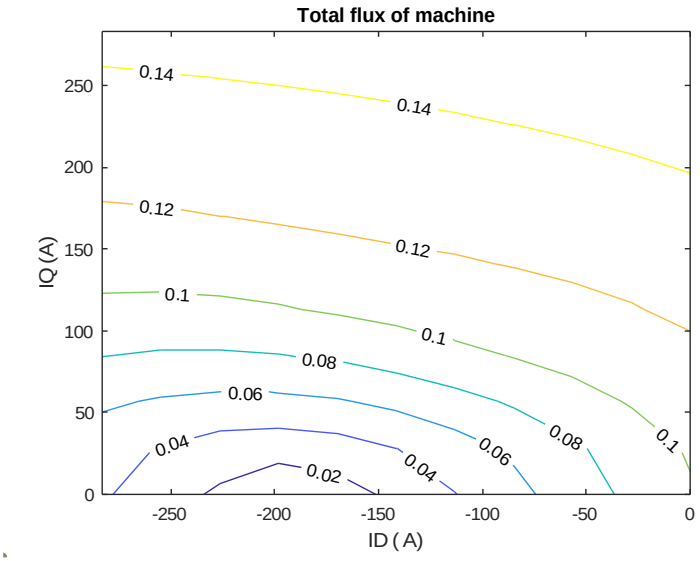


Figure B2. Flux of the machine ( Wb)

When knowing how the flux is affected by the current, the current needed to produce a certain torque is found via the program 'Find_a_current.m'. The program tries to find the best current combination that matches,

$$T_{ref} - \varepsilon < T_{calc} < T_{ref} + \varepsilon$$
$$\psi_{dq} < \psi_{max}$$
$$\psi_{max} = \frac{U_{dqmax}}{\omega_{el}}$$

and maximise the torque per ampere (MTPA).

$U_{dqmax}$ is the max voltage the converter can produce given a certain DC-link voltage and $\omega_{el}$ is the electric frequency. $T_{ref}$ is the set value of the routine and $\varepsilon$ is a small value.

The output of the program 'Find_a_current.m' is input to the final evaluation where the speed, torque and corresponding losses are found over the map, performed by the program 'Mapping_of_motor.m'.

Finally, the losses over the drive cycle may be found using the program 'WLTP_loss.m'.

# Appendix C Material data

Magnet data NMX37

Temperature 100 °C

Relative permeability 1.039

Coercitive force  -876 kA/m

Conductivity  625000 Siemens/m

NO30 Cogent

Kh 186.38

Kc 0.3229

Ke 0

Kdc 0

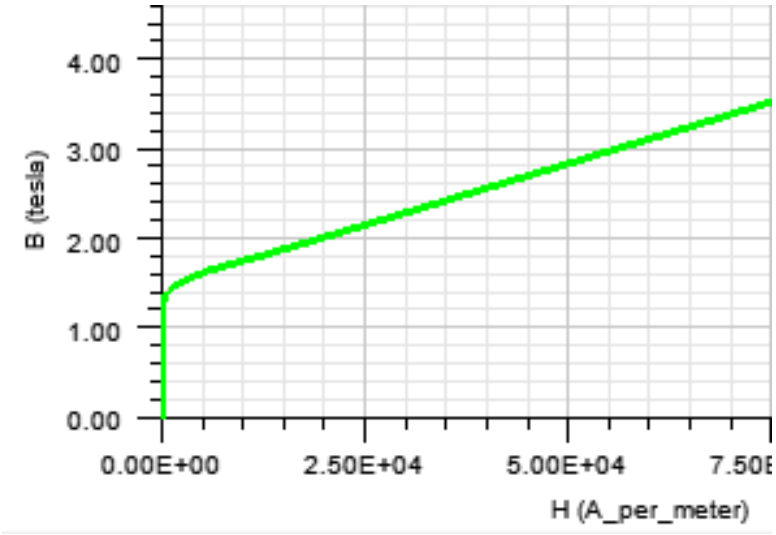


Somaloy 1000_5P

Kh 620.16

Kc 0.2976

Ke 6.381

Kdc 0

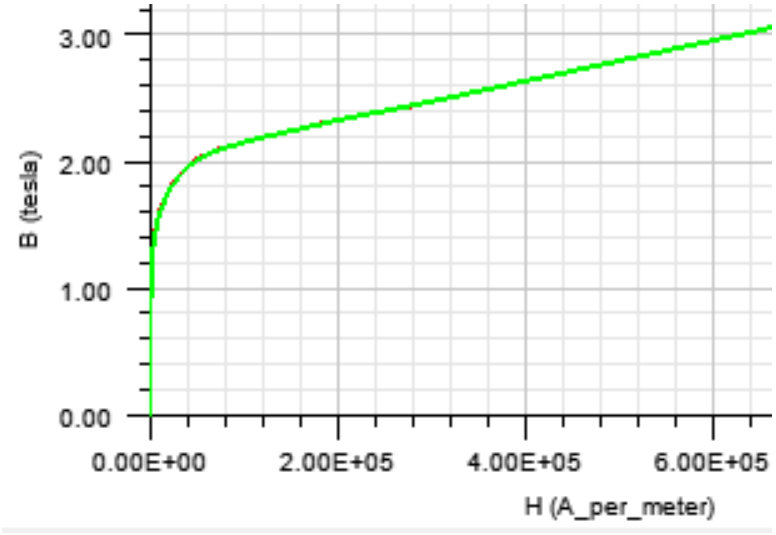

GO-mtrl

Kh 44.08

Kc 0.4237

Ke 0.6655

Kdc 0

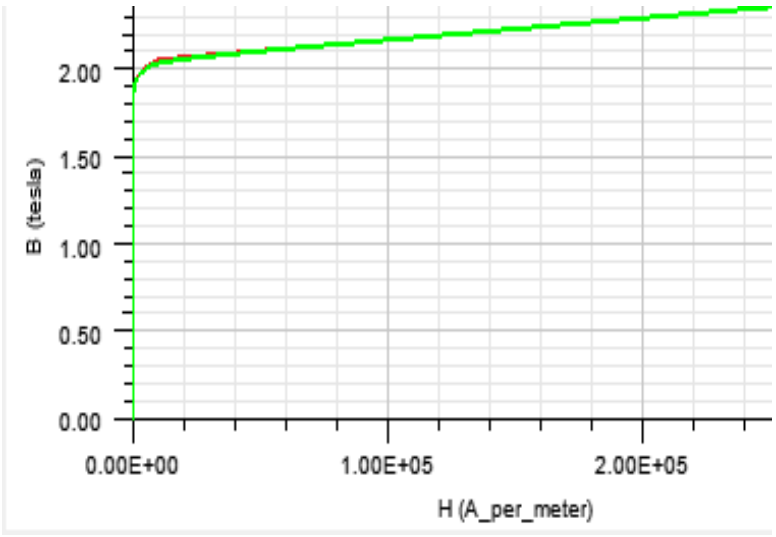

# Appendix D Summary of machine data

| | 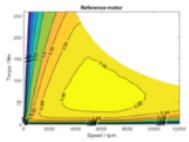 | 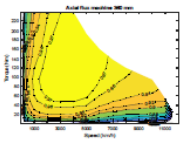 | 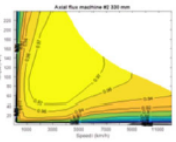 | 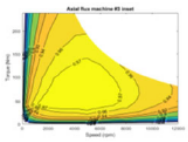 | 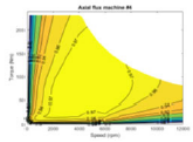 | 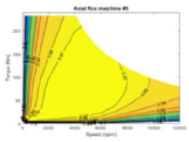 | 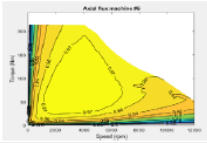 |
|---|---|---|---|---|---|---|---|
| Main data | Ref. machine | Machine #1 | Machine #2 | Machine #3 | Machine #4 | Machine #5 | Machine #6 |
| | v-PM, distr. wind. RFM | surface PM | smaller than #1,higher J | inset PM concentrated w. | inset PM distributed w. | Grain Oriented core | toroidal Wind. **Not finished** |
| Outer diameter | 200 mm | 360 mm | 320 mm | 310 mm | 310 mm | 310 mm | 294 mm |
| Inner diameter | 135 mm | 252 mm | 252 mm | 217 mm | 217 mm | 217mm | 206mm |
| Air gap | 0,75 mm | 1 mm (per side) | 0,7 mm (per side) | 0,9mm (per side) | 0,9mm (per side) | 0,8mm (per side) | 0,8mm (per side) |
| Number of poles | 8 | 10 | 10 | 10 | 10 | 10 | 10 |
| Number of slots | 48 | 15 | 15 | 15 | 30 | 30 | 30 |
| Stator length | 127 mm | 32 mm | 32 mm | 30 mm | 30 mm | 32 mm | 32 mm |
| Rotor length | 127 mm | 19,5 mm | 13 mm | 29,9 mm | 29,9 mm | 30,9 mm | 30,9 mm |
| Core material | NO30 | NO30 | NO30 | NO30 | NO30 | GO-mtrl | NO30 |
| Rotor material | | | | Somaloy 1000 | Somaloy 1000 | Somaloy 1000 | Somaloy 1000 |
| Slot data | Ref, machine | Machine #1 | Machine #2 | Machine #3 | Machine #4 | Machine #5 | Machine #6 |
| b0 | 2 mm | 3 mm | 3 mm | 3 mm | 3 mm | 3 mm | 3 mm |
| b1 | 5 mm | 20 mm | 17,8 mm | 16 mm | 8 mm | 8,0 mm | 7,0 mm |
| b2 | 5 mm | 20 mm | 17,8 mm | 16 mm | 8 mm | 8,0 mm | 7,0 mm |
| hs0 | | 1 mm | 1 mm | 1 mm | 1 mm | 1 mm | 1 mm |
| hs1 | | 1 mm | 1 mm | 1 mm | 1 mm | 1 mm | 1 mm |
| hs2 | 17 mm | 14 mm | 12,4 mm | 13 mm | 13 mm | 13, mm | 11, mm per half |
| Winding and magnet data | Ref, machine | Machine #1 | Machine #2 | Machine #3 | Machine #4 | Machine #5 | Machine #6 |
| Magnet thickness | 4,6 mm | 3,3 mm | 2,9 mm | 3,4 mm | 3,4 mm | 2,9 mm | 2,9 mm |
| Magnet width | 18 mm | 85 % of pole | 85 % of pole | 70 % of pole | 70 % of pole | 70 % of pole | 70 % of pole |
| Magnet material | NMX-37 | NMX-37 | NMX-37 | NMX-37 | NMX-37 | NMX-37 | NMX-37 |
| Magnet temp | 70 °C | 100 °C | 100 °C | 100 °C | 100 °C | 100 °C | 100 °C |
| Number of turns | 8 per slot | 20 per slot | 20 per slot | 22 per slot | 10 per slot | 9 per slot | 10 per slot |
| Fill factor | 45,00% | 53,00% | 52,60% | 52,60% | 52,60% | 52,60% | 52,60% |
| Turn length | | 198 mm | 223 mm | 192 mm | 297,3 mm | 311,3 mm | 104,8 mm |
| Copper diameter | | 3,1 mm | 2,8 mm | 2,6 mm | 2,8 mm | 3,14 mm | 3,2 mm |
| No, parallell con | 4 | 2 | 2 | 1 | 1 | 1 | 1 |
| $R_s$ ( Maxwell) | | 40 mΩ | 35,7 mΩ | 49,7 mΩ/half | 52,1mΩ/half | 42,2 mΩ/half | 15,8 mΩ/half |
| Mcu | 4,8 | 4,67 | 3,3 | 3 | 4,75 | 4,4 | 0,95 |
| Mstator | 11,8 | 9 | 6,42 | 6,44 | 6,39 | 7,82 | |
| Mnd | 1,26 | 2,16 | 1,5 | 1,36 | 1,36 | 1,16 | 1,08 |
| Mfer/Mrotor | 7,2 | 12,8 | 6,36 | 15,38 | 15,3 | 18,3 | 14,3 |
| Jcu @ 240 Nm | 20 A/mm2 | 12,4 A/mm2 | 13,7 A/mm2 | 20,3 A/mm2 | 20,5A/mm2 | 20,5 A/mm2 | 27,1 A/mm2 |
| pole shoe height | | | | 7 mm | 7 mm | 7,0 mm | 4,0 mm |
| Mteeth | | | | | | | 14,8 |
| Mcore | | | | | | | 8,7 |
| total weight | 25,1 | 28,6 | 17,6 | 26,2 | 27,8 | 31,7 | 39,8 |

Green fields show changes compared to previous design

Yellow fields show questionmarks

**DEPARTMENT OF Electrical Engineering**
**CHALMERS UNIVERSITY OF TECHNOLOGY**
Gothenburg, Sweden
www.chalmers.se

CHALMERS
UNIVERSITY OF TECHNOLOGY